Published in "Journal of Comparative Neurology 524(15): 2955–2981, 2016"
which should be cited to refer to this work.

The *Foxb1*-Expressing Neurons of the Ventrolateral Hypothalamic Parvafox Nucleus Project to Defensive Circuits

Alessandro Bilella,[1] Gonzalo Alvarez-Bolado,[2] and Marco R. Celio[1]*

[1]Anatomy Unit and Program in Neuroscience, Department of Medicine, Faculty of Sciences, University of Fribourg, CH-1700 Fribourg, Switzerland
[2]Institute of Anatomy and Cell Biology, University of Heidelberg, 69120 Heidelberg, Germany

ABSTRACT

The parvafox nucleus is an elongated structure that is lodged within the ventrolateral hypothalamus and lies along the optic tract. It comprises axially located parvalbumin (Parv)-positive neurons and a peripheral cuff of *Foxb1*-expressing ones. In the present study, injections of Cre-dependent adenoviral constructs were targeted to the ventrolateral hypothalamus of *Foxb1/Cre* mice to label specifically and map the efferent connections of the *Foxb1*-expressing subpopulation of neurons of the parvafox nucleus. These neurons project more widely than do the Parv-positive ones and implicate a part of the axons known to emanate from the lateral hypothalamus. High labeling densities were found in the dorsolateral and the upper lateral portion of the periaqueductal gray (PAG), the Su3 and PV2 nuclei of the ventrolateral PAG, the cuneiform nucleus, the mesencephalic reticular formation, and the superior colliculus. Intermediate densities of terminals were encountered in the septum, bed nucleus of the stria terminalis, substantia innominata, various thalamic and hypothalamic nuclei, pedunculopontine nucleus, Barrington's nucleus, retrofacial nucleus, and retroambigual nucleus. Scattered terminals were observed in the olfactory bulbs, the prefrontal cortex and the lamina X of the cervical spinal cord. Because the terminals were demonstrated to express the glutamate transporter VGlut2, the projections are presumed to be excitatory. A common denominator of the main target sites of the *Foxb1*-positive axons of the parvafox nucleus appears to be an involvement in the defensive reactions to life-threatening situations. The hypothalamic parvafox nucleus may contribute to the autonomic manifestations that accompany the expression of emotions.

INDEXING TERMS: PAG; anxiety; stress; defensive reaction; aggression; attack area; PV1 nucleus; PV1-Foxb1 nucleus; blood pressure control; respiration; vocalization

The lateral hypothalamus is a large, reticular region of the diencephalon. It is composed of a "confederation of scattered cells" (Peyron et al., 1998), which are involved in several physiological processes, ranging from the control of feeding to that of sleep (Saper, 2004). Interest in this part of the hypothalamus underwent a revival after the discovery therein of abundant scattered neurons expressing the peptide hypocretin/orexin (de Lecea et al., 1998; Sakurai et al., 1998b). Hypocretin/orexin-expressing cells are intermingled with MCH-positive ones (Skofitsch et al., 1985). The two populations play similar roles in the control of food intake and complementary ones in that of the sleep–wake cycle (Barson et al., 2013; de Lecea et al., 1998). The orexigenic function of the two peptides was revealed after intracerebral injections (Sakurai et al., 1998b), and the hypnagogic one after the detection of defective orexin receptors in narcoleptic dogs (Lin et al., 1999). These findings have been confirmed by tracing the axonal projections of the hypocretin/orexin- and MCH-expressing neurons (Peyron et al., 1998; Skofitsch et al., 1985). The excitatory projections

Grant sponsor: Swiss National Science Foundation; Grant number: 3100A0-11352.

*CORRESPONDENCE TO: Anatomy Unit and Program in Neuroscience, Department of Medicine, Faculty of Sciences, University of Fribourg, Rte A. Gockel 1, CH-1700 Fribourg, Switzerland. E-mail: marco.celio@unifr.ch

of the hypocretinin/orexin-positive cells to the locus coeruleus (Peyron et al., 1998) highlight their role in arousal and wakefulness (Sutcliffe and de Lecea, 2000). What is remarkable in this unparalleled success story is the unusual way in which the functional roles of the nerve cell aggregates in the lateral hypothalamus were unfolded. In most other cases, the path of discovery begins with the application of classical Nissl-staining techniques, whereby subtle cytoarchitectonic differences are revealed. Later, the connections are mapped using precise stereotactic tracer techniques (see, e.g., Hahn and Swanson, 2015). From these meticulous connectivity studies, the probable functions of individual cytoarchitectonic regions can then be deduced. For example, the connections of the juxtaventromedial region of the lateral hypothalamus point to a prominent role in reproductive behavior (Hahn and Swanson, 2015). Hence, both the "unique" peptide approach and the Nissl-stereotactic tracer injection one have been useful in elucidating the roles of subpopulations of neurons or of subareas in the lateral hypothalamus.

Using a combination of the two approaches, viz. by injecting Cre-dependent tracers into Parv/Cre mice and by monitoring the expression of the nonunique marker parvalbumin (Parv), we have mapped the connections of the Parv-positive string of neurons in the PV1 nucleus (Celio et al., 2013), which is embedded in the medial forebrain bundle (mfb) of the ventrolateral hypothalamus. Later, the existence of a cuff of Foxb1-expressing neurons was revealed around the Parv-expressing ones (Bilella et al., 2014). Taking this circumstance into account, the PV1 nucleus was thenceforth referred to as the parvafox nucleus (Alvarez-Bolado and Celio, 2015). *Foxb1* is a transcription factor gene of the forkhead family. It is expressed predominantly in the cell nucleus and is absent from the dendrites and the axons (Alvarez-Bolado et al., 2000a,b; Kaestner et al., 1993; Radyushkin et al., 2005; Wolf and Ryu, 2013; Zhao et al., 2008). *Foxb1* is expressed not only in neurons of the parvafox nucleus but also in those of the mammillary nuclei (Zhao et al., 2008). The aim of the present study was to trace the projections of the cuff of *Foxb1*-expressing neurons of the parvafox nucleus after the stereotactic injection into *Foxb1/Cre* mice of Cre-dependent adeno-associated viral constructs that selectively target this group of cells.

The *Foxb1*-expressing neurons were found to project heavily to a number of brain sites that are known to be involved in defensive behavior. The influence exerted by the *Foxb1*-expressing component of the parvafox nucleus on these brain regions may relate to the autonomic concomitants of the defensive responses for which these regions are renowned.

MATERIALS AND METHODS

The animals used in this study were *Foxb1-Cre* mice, in which the Foxb1-immunopositive neurons coexpress the enzyme Cre-recombinase and EGFP (Zhao et al., 2007). The animals were subjected to a 12-hour dark/12-hour light cycle, maintained at a constant temperature (24°C), and fed ad libitum. The study was performed in accordance with the regulations of the Swiss animal experimentation law (permissions 26-10, 27-10, 2013_04_FR, and 2013_05_FR).

Tract-tracing experiments

Sixteen mice, weighing 25–30 g, were anesthetized with a mixture of Ketalar (Parke-Davis, Ann Arbor, MI; 75 mg/kg body weight) and xylazine (Streuli, Uznach, Switzerland; 10 mg/kg body weight). The adenoviral anterograde tracers were injected in a volume of 20 nl from a Hamilton syringe, which was connected to a stereotactic apparatus (Kopf, Tujinga, CA). The injections into the right lateral hypothalamus were made at the following coordinates: rostrocaudal Bregma −1.5 mm, mediolateral −1.4 mm, dorsoventral −5.5 mm. The viral constructs included: AAV2/1.CAG.FLEX.EGFP.WPRE.bGH, which was injected into 10 mice (see Table 2;

Abbreviations

1	layers, tenia tecta
3v	third ventricle
4v	fourth ventricle
7N	facial nucleus
10N	dorsal motor nucleus of vagus
12N	hypoglossal nucleus
A1	noradrenaline cells
A13	A13 dopamine cells
AAD	anterior amygdaloid area, dorsal part
AAV	anterior amygdaloid area, ventral part
ac	anterior commisure
aca	anterior commissure, anterior
Acb	accumbens nucleus
Acbc	accumbens nucleus, core
AcbSh	accumbens nucleus, shell
ACo	anterior cortical nucleus
AD	anterodorsal thalamic nucleus
AHA	anterior hypothalamic area, anterior part
AHC	anterior hypothalamic area, central
AHP	anterior hypothalamic area, posterior
AIV	agranular insular cortex, ventral part
Amb	ambiguous nucleus
Ambc	ambiguous nucleus, pars compacta
AmbL	ambiguous nucle, loose
ant	anterior hypophysis
AOB	accessory olfactory bulb
AOD	anterior olfactory area, dorsal part
AOE	anterior olfactory area, external part
AOL	anterior olfactory area, lateral part
AOM	anterior olfactory nucleus, medial
AOV	anterior olfactory nucleus, ventral
Arc	arcuate nucleus

AVDM	anteroventral thalamic nucleus, dorsomedial
AVPO	anteroventral preoptic nucleus
aq	aqueduct
Bar	Barrington's nucleus
Bö	Bötzinger complex
BST	bed nucleus of the stria terminalis
BSTL	bed nucleus of the stria terminalis, lateral division
BSTMA	bed nucleus of the stria terminalis, medial division, anterior part
BSTMPI	bed nucleus of the stria terminalis, medial division, posterointermediate part
BSTMPL	bed nucleus of the stria terminalis, medial division, posterolateral part
BSTV	bed nucleus of the stria terminalis, ventral division
C1	adrenaline cells
CC	central canal
Ce	central amygdaloid nucleus
CeM	central amygdaloid nucleus, medial division
CGA	central gray, alpha part
CGPn	central gray pons
CI	inferior colliculus
CL	central lateral thalamic nucleus
CM	central medial thalamic nucleus
CnF	cuneiform nucleus
CPu	caudate putamen (striatum)
Cu	cuneate nucleus
DG	dentate gyrus
dlPAG	dorsolateral periaqueductal gray
DM	dorsomedial hypothalamic nucleus
DMTg	dorsomedial tegmental area
DMV	dorsomedial hypothalamic nucleus, ventral part
DP	dorsal peduncular cortex
DpG	deep gray layer, sup colliculus
DPGi	dorsal paragigantocellular nucleus
DpMe	deep mesencephalic nucleus
DR	dorsal raphe nucleus
DRV	dorsal raphe nucleus, ventral part
DTgC	dorsal tegmental nucleus, central
DTgP	dorsal tegmental nucleus, pericentral
DTT	dorsal taenia tecta
dVLM	dorsoventrolateral reticular nucleus
EPl	external plexiform layer of the olfactory bulb
f	fornix
Fr	fasciculus retroflexus
FrA	frontal association cortex
g7	genu facial nerve
gcc	genu corpus callosum
Gem	gemini hypothalamic nucleus
Gi	gigantocellular reticular nucleus
GlA	glomerular layer of the accessory olfactory bulb
Gr	gracile nucleus
GrO	granular cell layer of the olfactory bulb
HDB	nucleus of the horizontal limb of the diagonal band
Hi	hippocampus
icp	inferior cerebellar peduncle
InG	intermediate gray layer of the superior colliculus
InWh	intermed white layer sup colliculus
IOM	inferior olive, medial nucleus
IRt	intermediate reticular nucleus
LA	lateroanterior hypothalamic nucleus
LC	locus coeruleus
LDTg	laterodorsal tegmental nucleus
LH	lateral hypothalamic area
LHb	lateral habenular nucleus
LM	lateral mammillary nucleus
LO	lateral orbital cortex
LPAG	lateral periaqueductal gray
LPB	lateral parabrachial nucleus
LPGi	lateral paragigantocellular nucleus
LPO	lateral preoptic area
LRt	lateral reticular nucleus
LS	lateral septal nucleus
LSD, LSV	lateral septal nucleus, dorsal, ventral parts
LSI	lateral septal nucleus, dorsal, resp ventral parts
LV	lateral ventricle
LVe	lateral vestibular nucleus
MCPO	magnocellular preoptic nucleus
MDC	mediodorsal thalamic nucleus, central
MDL	mediodorsal thalamic nucleus, lateral
MDM	mediodorsal thalamic nucleus, medial
MdV	medullary reticular nucleus
ME	median eminence
MeA	medial amygdalar nucleus, anterior
MeAD	medial amygdalar nucleus, anterodorsal
MeAV	medial amygdalar nucleus, anteroventral
MePD	medial amygdalar nucleus, posterodorsal
MePV	medial amygdalar nucleus, posteroventral
mfb	medial forebrain bundle
mlf	medial longitudinal fascicle
MnR	medial raphe nucleus
MO	medial orbital cortex
MPA	medial preoptic area
MPB	medial parabrachial nucleus
MPOA	medial preoptic area, anterior
MRe	mammillary recess, 3rd ventricle
mt	mammillothalamic tract
mtg	mammillotegmental tract
MVe	medial vestibular nucleus
MVePC	medial vestibular nucleus, parvicellular part
NRTh	reticular thalamic nucleus
NTS	nucleus of the solitary tract
Nv	navicular postolfactory nucleus
Op	optic nerve layer superior colliculus
opt	optic tract
OV	olfactory part of lateral ventricle
Pa	paraventricular hypothalamic nucleus
PAG	periaqueductal gray
PaLM	paraventricular hypothalamic nucleus lateral magnocellular part
PC	paracentral thalamic nucleus
PCRt	parvicellular reticular nucleus
PCRtA	parvicellular reticular nucleus, alpha part
PDTg	posterodorsal tegmental nucleus
PF	parafascicular thalamic nucleus
PFA	paraformaldehyde
PH	posterior hypothalamic area
PLH	peduncular part lateral hypothalamus
PMD	premammilary nucleus, dorsal
PMV	premammilary nucleus, ventral part
PnC	pontine reticular nucleus, caudal part
Post	posterior hypophysis
PPTg	pedunculopontine nucleus
Pr	prepositus nucleus
PrBö	pre-Bötzinger complex
PrL	prelimbic cortex
PSTh	parasubthalamic nucleus
PV	paraventricular thalamic nucleus
PV2	parvalbumin-positive nucleus 2
PVA	paraventricular thalamic nucleus, anterior
PVP	paraventricular thalamic nucleus, posterior
PVT	paraventricular thalamic nucleus
Re	reuniens thalamic nucleus
Rf	fasciculus retroflexus
Rh	rhomboid thalamic nucleus
RMg	raphe magnus nucleus
RpN	raphe pontis nucleus
RVL	rostroventrolateral medulla reticular nucleus
SC	superior colliculus
SHi	septohippocampal nucleus
SI	substantia innominata
SOlCe	solitary nucleus, central part
sp5	spinal trigeminal tract
Sp5C	spinal trigeminal nucleus, caudal part
Sp5I	spinal trigeminal nucleus, interpolar part
Su3	supraoculomotor nucleus of the PAG
Sub	submedius thalamic nucleus
SuM	supramammillary nucleus
SuML	supramammillary nucleus, lateral part
VA	ventral anterior thalamic nucleus
VDB	nucleus vertical limb diagonal band
Virg	virgola
vlPAG	ventrolateral PAG
VLTe	ventrolateral tegmental nucleus
VM	ventromedial thalamic nucleus
VMHC	ventromedial hypothalamic nucleus, central
VMHDM	ventromedial hypothalamic nucleus, dorsomedial
VMHVL	ventromedial hypothalamic nucleus, ventrolateral
VO	ventral orbital cortex
VP	ventral pallidum
VRe	ventral reuniens thalamic nucleus
Vsc	ventrospinocerebellar tract
VTA	ventral tegmental area
VTg	ventral tegmental nucleus (Gudden)
VTM	ventral tuberomammilary nucleus
ZI	zona incerta

TABLE 1.

Antisera and Antibodies Used in This Study[1]

Antibody	Structure of immunogen	Manufacturer, catalog No.	Dilution factor	RIID
Antiparvalbumin	Purified carp parvalbumin	SWant, lot 10-11F, PV235	1: 1,000	AB_10000343
Anti-GFP	Jellyfish (*Aequorea victoria*)	Life Technologies, lot A64551, rabbit polyclonal	1:2,000	AB_221570
Anti-VGluT1	Strep-Tag fusion protein of rat VGLUT 1 (aa 456–560)	Synaptic Systems, 135 403, rabbit polyclonal	1:30,000	AB_887883
Anti-VGluT2	Strep-Tag fusion protein of rat VGLUT 2 (aa 510–582)	Synaptic Systems, 135403, rabbit polyclonal	1:30,000	AB_2315570
Anti-GAD67	Purified mouse monoclonal IgG2a in buffer containing 0.1% sodium azide	Millipore, MAB5406	1:1,000	AB_2278725
TH	TH purified from rat PC12 cells	Immunostar, 22941, lot 1241002, mouse monoclonal	1:3,000	AB_572268
nNOS	Lyophilized whole-serum IgG	Immunostar, rabbit polyclonal, 24287, lot 741001	1:2,000	AB_572256

[1]Well characterized antibodies were acquired from various commercial sources.

194/13, 195/13, 249/13, 9/15, 10/15, 180/15, 182/15, 183/15, 25/16, 26/16), and AAV2/1.CAG.FLEX.Tomato.WPRE.bGH, which was injected into eight mice (see Table 2; 307/13, 392/14, 9/15, 10/15, 131/15, 180/15, 25/16, 26/16). The constructs were developed at the Allen Institute and are commercially available from the Vector Core at the University of Pennsylvania (http://www.med.upenn.edu/gtp/vectorcore/).

Four weeks after the injections, the mice were transcardially perfused first with physiological (0.9%) saline and then with a 4%- solution of paraformaldehyde in 0.1M phosphate buffer, [(PB) pH 7.3]. The brains and the spinal cords were excised, immersed overnight in the same fixative, and then transferred for cryoprotection to a chilled solution of 30% sucrose (4°C). Forty-micrometer-thick coronal, parasagittal and horizontal cryosections were prepared with a freezing microtome (Reichert-Jung, Vienna, Austria) and collected in PB.

Immunohistochemistry

In some tracing experiments, free-floating sections were exposed for 2 days at 4°C to a rabbit anti-GFP antiserum (Life Technologies, Japan; catalog No. A6455, RRID:AB_221570; diluted 1:3,000 in Tris-buffered saline [TBS] containing 0.2% Triton X-100 and 10% bovine serum). The sections were rinsed in TBS and then exposed for 2 hours at room temperature to the anti-rabbit biotinylated secondary antibody (Vector Laboratories, Burlingame, CA; diluted 1:200 in TBS + 10% bovine serum). After rinsing once in TBS and twice in Tris-HCl (pH 8.2), the sections were exposed for 2 hours to Alexa 488-conjugated streptavidin (Jackson Immunoresearch; diluted 1:500 in Tris-HCl, pH 8.2). To identify the region of the parvafox nucleus, all sections were subsequently exposed, in parallel, for 1 day at room temperature to a primary monoclonal antibody against Parv (PV235; SWant, Marly, Switzerland; catalog No. 235, RRID:AB_10000343; diluted 1:1,000 in TBS + 0.2% Triton X-100 + 10% bovine serum) and then for 2 hours to an anti-mouse Cy3 antibody (Jackson Immunoresearch; diluted 1:200 in Tris-HCl, pH 8.2).

To reveal the neurotransmitter used by the terminals, antisera against the glutamate transporters VGlut1 and VGlut2 (Synaptic Systems, Göttingen, Germany; catalog No. 135 403, RRID:AB_887883; Synaptic Systems, catalog No. 135 103 RRID:AB_2315570) and the GABA-synthesizing enzyme GAD67 (Millipore, Darmstadt, Germany; catalog No. MAB5406, RRID:AB_2278725) were employed. To identify the catecholaminergic sites, antibodies against tyrosine hydroxylase (TH; Immunostar, Hudson, WI; catalog No. 22941, RRID:AB_572268) were used. To identify the dLPAG, an antiserum against the neuronal nitric oxide synthase (nNOS; Immunostar; catalog No. 24287, RRID:AB_572256) was employed (Table 1).

Cell nuclei were sporadically revealed by counterstaining with DAPI (diluted 1:2,000 in phosphate-buffered saline) for 5 minutes at room temperature. The sections were mounted and evaluated in a Leica 6000 epifluorescence microscope (equipped with a Hamamatsu C4742-95 camera), a digital slide scanner (Nanozoomer, Hamamatsu), or a Leica TCS SP5 confocal laser microscope.

The images were postprocessed for brightness and contrast in Adobe Photoshop CS5. The image stacks were prepared with ImageJ 1.44p (RRID:SCR_003070), and the figures were collated in the Adobe Illustrator CS6 (RRID:SCR_014198).

TABLE 2.

Distribution of Labeled Axons and Terminals in the Brain After Injection of Cre-Dependent Tracers in the Ventrolateral Hypothalamus of *Foxb1-Cre* Mice[1]

Brain area	Region	Stained fibers	Terminals	Other injections
Telencephalon	Lateral septum, ventral (LSV)		+	
	Lateral septum, intermediary (LSI)		+	
	Accessory olfactory bulb (AOB)		++	
	Anterior olfactory area, dorsal part (AOD)		++	
	Anterior olfactory area, external part (AOE)		++	
	Anterior olfactory area, lateral part (AOL)		++	
	Anterior olfactory area, medial part (AOM)		++	
	Granular cell layer olfactory bulb (GrO)		++	
	Lateral orbital cortex (LO)		+	
	Medial orbital cortex (MO)		+	
	Ventral orbital cortex (VO)		+	
	Nucleus of the stria medullaris (SM)	+	+	
	Substantia innominate (SI)	(+)	(+)	
Thalamus	Anterodorsal thalamic nucleus (AD)		(+)	+++ 195-13
	Anterodorsal tegmental nucleus (AVDM)		+	
	Centromedial thalamic nucleus (CM)		+	
	Central thalamic nucleus (CL)		+	
	Field of Forel (FF)		+	
	Mediodorsal thalamic nucleus, central (MDC)		+	
	Medial habenular nucleus (MHB)		++	
	Paraventricular hypothalamic nucleus lateral magnocellular part (PALM)	++	++ Bilat	
	Parafascicular thalamic nucleus (PF)		++	
	Prerubral nucleus (PR)		+	
	Precommissural nucleus (PrC)		++ Bilat	
	Periventricular fiber system (Pv)	+++		
	Paraventricular thalamic nucleus (PV)		+	
	Paraventricular thalamic nucleus, anterior (PVA)			
	Paraventricular thalamic nucleus, posterior (PVP)		++	
	Reuniens thalamic nucleus (Re)		+	
	Submedius thalamic nucleus (SUB)		++	
	Zona incerta (bilateral) (ZI)	++	++ bilat	
Hypothalamus	Anterior hypothalamic area, anterior and posterior (AHA and AHP)		+	
	Gemini hypothalamic nucleus (Gem)		+++	
	Lateroanterior hypothalamic nucleus (LA)	(+)	(+)	
	Lateral hypothalamus (LH)	++	++	
	Magnocellular preoptic nucleus (MCPO)	++	++	
	Medial forebrain bundle (mfb)	++		
	Parasubthalamic nucleus (PSTh)		+++	
	Tuber cinereum (TC)	+	++	
	Ventral tuberomammillary nucleus (VTM)		++	
Mesencephalon	Cuneiform nucleus (CnF)		+++	
	Kölliker-Fuse nucleus (KF)			++ 9-15 Red 246-15
	Dorsolateral periaqueductal gray (dLPAG)		++	
	Lateral periaqueductal gray (lPAG)		+++	
	Deep mesencephalic nucleus (DpMe)		+++	
	Parvalbumin nucleus 2 (PV2)		+++	
	Peduncolopontine tegmental nucleus (PPTg)		++	
	Supraoculomotor nucleus (Su3)		+++	
	Ventrolateral nucleus (VL)		+	
Superior colliculus	Deep gray layer (DpG)		++	
	Intermediate gray layer (InG)		++	
	InWh intermediate white layer	++		
	Posterior pretectal nucleus, olivary pretectal nucleus (PPT, OPT)	+	++	
Tegmentum	Barrington (Bar)		++	

TABLE 2. *Continued*

Brain area	Region	Stained fibers	Terminals	Other injections
	Central gray, alpha and beta (Cga and CgB)		+	
	Central gray pons (CgP)		+	
	Dorsal tegmental nucleus, central (DTgC)		++	
	Dorsal tegmental nucleus, pericentral (DTgP)		++	
	Locus coeruleus (LC)		+	
	Laterodorsal tegmental nucleus (LDTg)		++	
	Microcellular tegmental nucleus (MiTg; border)		++	
	Posterodorsal tegmental nucleus (PDTg)		++	
	Pontine reticular nucleus caudal (PnC)	++	+	
	Sublaterodorsal nucleus (SUL)		+	
	Ventral tegmental area (VTA)	++	+	
Metencephalon	Medial lemniscus (ml)	++		
	Dorsal paragigantocellular nucleus (DPGi)		++	
	Deep mesencephalic nucleus (DpMe)	++	+	
	Gigantocellular nucleus (Gi)	+	+	
	Intermediate reticular nucleus (IRt)		++	
	Lateral paragigantocellular nucleus (LpGi)		+	
	Lateral reticular nucleus (LRt)		++	
	Lateral vestibular nucleus (LVe)	+		
	Med reticular nucleus dorsal (MdD)	+	+	
	Medial vestibular nucleus, parvicellular (MVePC)	+		
Myelencephalon	Pontine reticular nucleus (PnC)		(+)	
	Pedunculopontine tegmental nucleus (PpTn)		++	
	Nucleus retroambiguus (Ramb)		++	
	Spinal trigeminal nucleus, interpolar part (Sp5I)	+		

[1]The brain areas in which terminals and/or axons arising from the site of the injections in the lateral hypothalamus have been observed through the caudal and the rostral part of the brains (+) very low density. +, Low density; ++, high density; +++, very high density.

Characterization of the antisera

The monoclonal antiserum against Parv (SWant; catalog No. PV235) recognizes only one band (corresponding to a molecular weight of 12 kD) in Western blots of brain extracts that have been derived from various species, including rats and mice. The pattern of staining in the brain was consistent with previously documented findings (Celio, 1990). No staining is observed in the brains of Parv knockout mice (Schwaller et al., 1999).

The antiserum against GFP (Life Technologies; catalog No. A6455) was raised against the full-length recombinant molecule. Staining was observed only in the parvafox nucleus of the ventrolateral hypothalamus and in the mammillary nuclei. In other parts of the brain of animals that had been injected with a GFP-bearing viral construct for tracing, the pattern of distribution accorded with the expected one.

The specificity of the antiserum against VGlut2 (Synaptic Systems; catalog No. 135 403) was demonstrated by Western blot analysis of homogenized rat brains and/or crude synaptic vesicle in which a single, broad band corresponding to a molecular weight slightly above 60 kD was manifested and by preadsorbing the sections with the GST fusion protein that was used as an immunogen, which abolished all immunoreactivity (Zhou et al., 2007).

The specificity of the antiserum against VGlut1 (Synaptic Systems; catalog No. 135 302) has been demonstrated by Western blot analysis of homogenized rat brains and/or crude synaptic vesicle fractions from rat brain, in which a single, broad band slightly above 60 kD was found, and by preadsorption experiments with the GST fusion protein used as immunogen, in which the immunostaining of rat brain sections was completely eliminated (as for VGlut 2)

The specificity of the antiserum against glutamic acid decarboxylase 67 (GAD67; Millipore; catalog No. MAB5406) has been demonstrated by the reaction with the 67-kD isoform of glutamate decarboxylase (GAD67) of rat, mouse, and human origins (other species not yet tested). No detectable cross-reactivity with GAD65 by Western blot on rat brain lysate compared with blot probed with AB1511 that reacts with both GAD65 and GAD67 was seen.

The specificity of the antiserum against tyrosine hydroxylase (TH; Immunostar; catalog No. 22941) has been demonstrated with standard immunohistochemical methods. The antiserum demonstrates significant labeling of rat catecholamine neuron systems via the indirect immunofluorescent and biotin/avidin-HRP techniques. The antibody recognizes the 34-kD catalytic core of TH.

The antiserum against neuronal nitric oxide synthase (nNOS; Immunostar; catalog No. 24287, lot 741001) was tested by using standard immunohistochemical

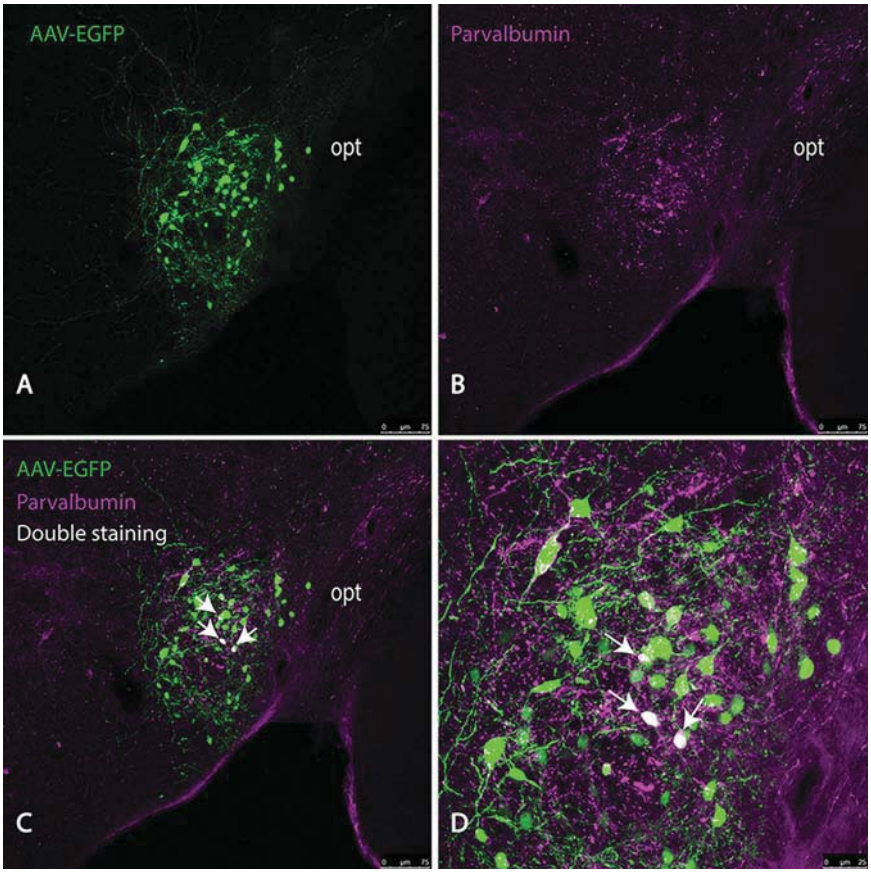

Figure 1. Confocal images of a cluster of *Foxb1/Cre*-expressing neurons in the ventrolateral hypothalamus after a stereotactic injection of the Cre-dependent AAV-EGFP construct. **A:** EGFP is expressed in the perikarya, the dendrites, and the axons of a large number of small cells. **B:** The Parv-immunopositive neurons are located within the bounds of the cluster of AAV-EGFP-labeled cells and are less numerous than these. **C:** A few of the neurons manifest dual coloring (arrows), which indicates that AAV-EGFP and Parv are colocalized. **D:** In this higher magnification view of C, the double staining is clearly visible (injection 195/13). Scale bars = 75 μm in A–C; 25 μm in D.

TABLE 3.

Quantification of Labeled Neurons in Four Injections[1]

	Mouse line	Marker	Region	Estimated population (using the mean section thickness	CE
194/13	Foxb1/Cre	AAV2/1-Cre virus	vLH	1,027.05	0.10
195/13	Foxb1/Cre	AAV2/1-Cre virus	vLH	879.14	0.10
249/13	Foxb1/Cre	AAV2/1-Cre virus	vLH	339.88	0.16
307/13	Foxb1/Cre	AAV2/1-Cre virus	vLH	1,206.34	0.11

[1]The mean total number of cells that took up the AAV2/1-Cre-dependent virus in the lateral hypothalamic parvafox nucleus of the *Foxb1/Cre* mice was estimated by using the optical fractionator. Given that the total number of Foxb1-expressing neurons in the parvafox nucleus has been estimated to be 1,200 (Bilella et al., 2014), almost all were infected with the virus in experiments 194/13 and 307/13.

methods. The antiserum worked properly for rat hypothalamus, striatum, cortex, and spinal cord as judged from indirect immunofluorescent and biotin/avidin-HRP techniques. Western blot analysis of brain homogenates shows the antibody specifically labels a band of approximately 155 kD. Immunolabeling is completely abolished by preadsorption with synthetic human nNOS (1419–1433) at 5 μg/ml of diluted antibody. No cross-reactivity with other forms of NOS was observed.

Cell counting

In four mice, the *Foxb1*/EGFP-positive neurons that took up the viral vectors were counted using the optical fractionator (West et al., 1991). This quantification was performed with in Stereoinvestigator 10.52 (MBF-Bioscience, Williston, VT; RRID:SCR_002526) mounted on a Zeiss photomicroscope (equipped with Hamamatsu Orca 0G5 camera). Counts were made on a uniform random systematic sample of every fourth coronal section. For

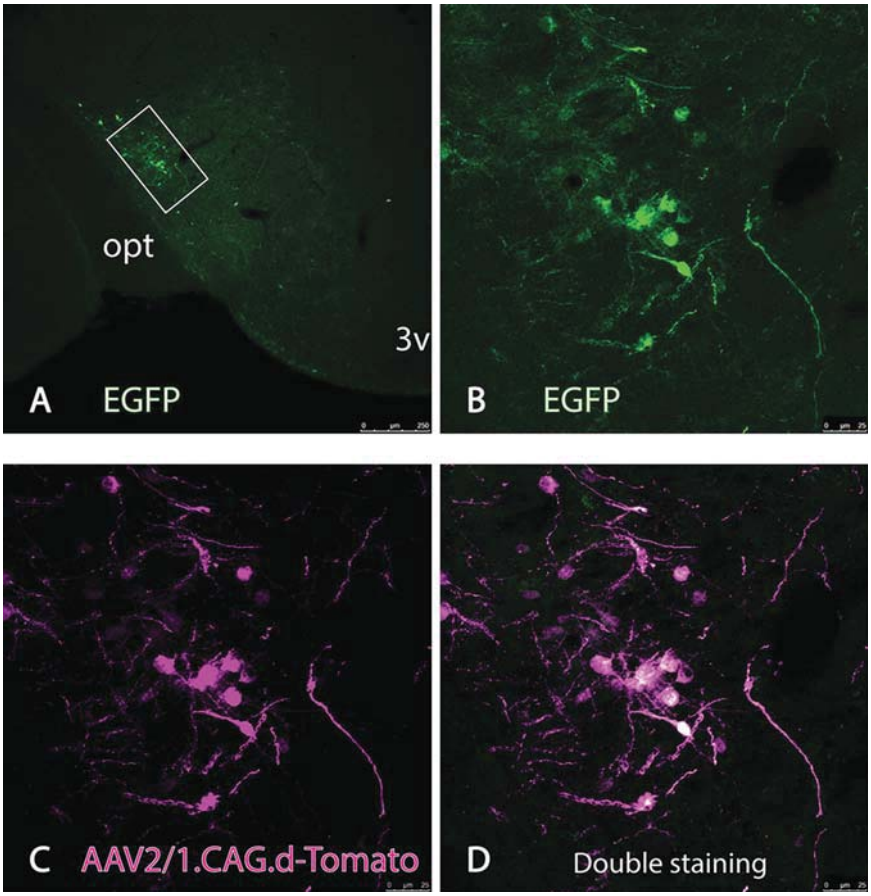

Figure 2. Confocal images of the parvafox nucleus after a stereotactic injection of the AAV-dTomato construct. **A:** Overview of the nucleus after exposure to an antibody against EGFP. The presence of intrinsic EGFP is thereby revealed. **B:** Higher magnification view of A. **C:** dTomato is expressed in the soma, the dendrites, and the axons of the *Foxb1/EGFP*-expressing neurons in the parvafox nucleus. **D:** Dual staining for Foxb1 and EGFP is clearly visible, attesting to the high specificity of the viral vector for the *Foxb1*-expressing neurons (injection 307/13). Scale bars = 250 μm in A; 25 μm in B–D.

the stereological estimations, the region of interest on the sections was first delineated. A counting frame of 70 × 70 μm was placed at 100-μm intervals along the x- and the y-axes of the section. The grid size was adapted to achieve an acceptable coefficient of error (CE; see below). At each counting site, the thickness of the section was estimated to be 30 μm.

The CE expresses the precision of the estimate (Slomianka and West, 2005). An average CE value of less than 0.15 was deemed to be appropriate for the present study. The adopted sampling scheme yielded on average CE of 0.12 (Table 2). To ensure that most of the variance across the animals was attributable to the experimental manipulations and to biological variation (but not to the estimation of the cell number), the CE^2/CV^2 ratio was calculated. Less than 10% of the variance across the animals ($CE^2/CV^2 = 0.085$) originated from the estimation of cell number.

RESULTS

Injection cases

In 13 of the 16 *Foxb1*-EGFP/Cre mice, the injections precisely hit the region of the lateral hypothalamus in which the *Foxb1*-expressing neurons were located (injections 194/13, 195/13, 249/13, 307/13, 392/14, 9/15, 10/15, 131/15, 180/15, 182/15, 183/15, 25/16, 26/16; see Table 2). In the remaining three cases, the injections were slightly too lateral, too medial, or too distal and also hit the mammillary bodies. These three brains served as controls. The most comprehensive analyses were performed on five representative data sets that implicated the parvafox nucleus most exclusively (injections 194/13, 9/15, 10/15, 131/15, 180/15).

Labeled cell bodies were restricted to the ventrolateral hypothalamus (Fig. 1A), namely, to the region in which the parvafox nucleus is located, as revealed by

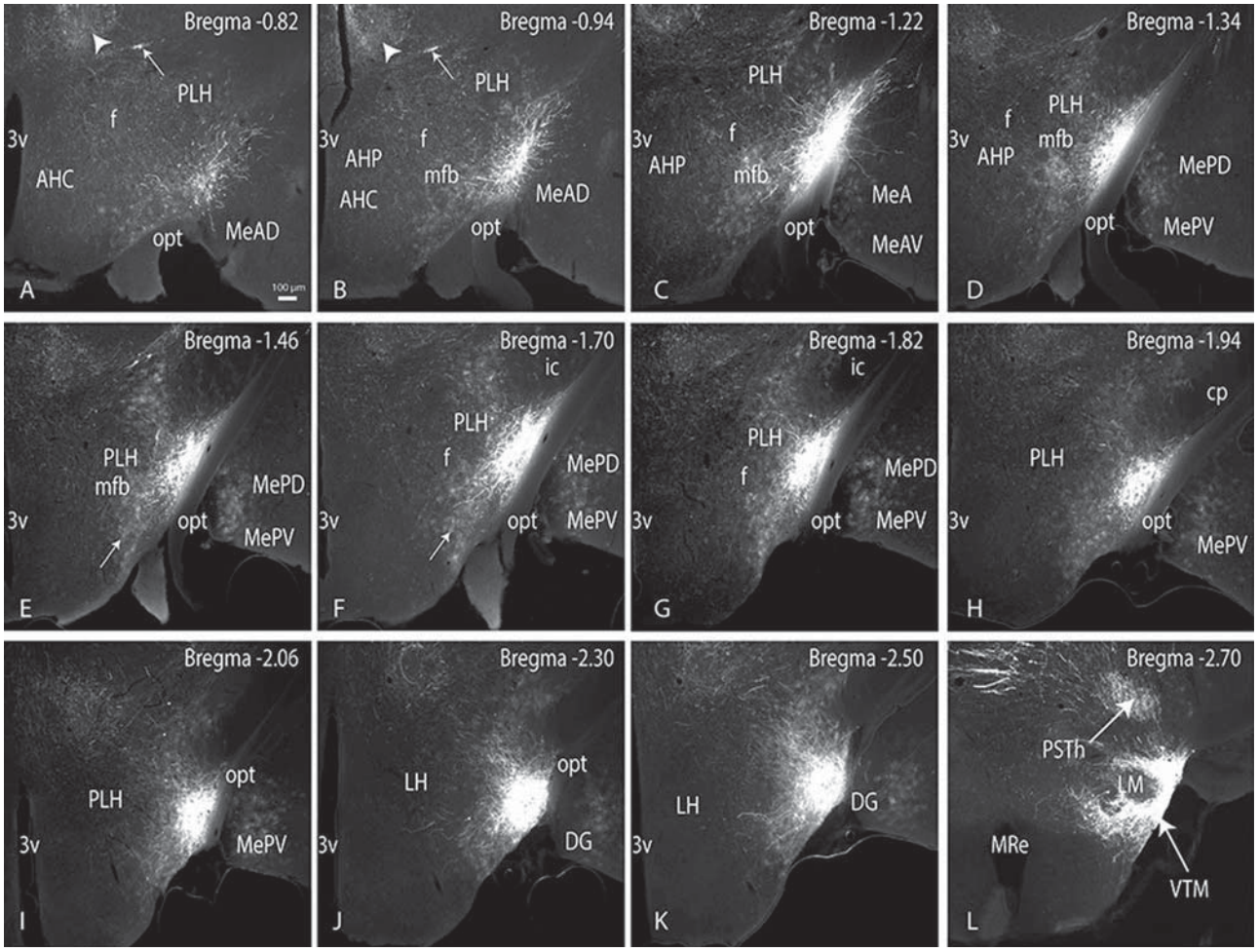

Figure 3. Epifluorescent images of 12 consecutive coronal sections through the parvafox nucleus, which was cut in a rostral (A)-to-caudal (L) direction [Bregma ~ −0.82 mm (A) to Bregma ~ −2.70 mm (L)]. The Cre-dependent AAV-EGFP has been taken up by the perikarya and fills the dendrites and the axons of the *Foxb1/Cre*-expressing cells. **A,B:** Parvafox nucleus, proximal portion. Only few *Foxb1*/Cre-expressing neurons are visible. The axons from the nucleus run throughout the lateral hypothalamus and reach the zona incerta (arrow) and the ventral thalamic nucleus (arrowhead) giving rise to descending and ascending bundle of fibers, respectively (Bregma ~ −0.82 mm, Bregma ~ −0.94 mm). **C–E:** The Foxb1-Cre-expressing neurons send axons that spread in all directions; fibers pass through the peduncular part of the lateral hypothalamus (PLH), and most of them flow into the medial forebrain bundle reaching several brain regions (Bregma ~ −1.22 mm, Bregma ~ −1.34 mm, Bregma ~ −1.46 mm). **F,G:** Middle portion of the parvafox nucleus. The neurons send projections in all directions; bundles of fibers run around the internal capsule, and others run in the same direction of the nucleus (Bregma ~ −1.70 mm, Bregma ~ −1.82 mm). **H–K:** Four consecutive sections through the most distal portion of the parvafox nucleus. The *Foxb1*/Cre-expressing neurons send projections in different directions (Bregma ~ −1.94 mm, Bregma ~ −2.50 mm). **L:** This panel shows only the dense bundle of fibers that run around the lateral mammillary nucleus (LM), throughout the ventral tuberomammillary nucleus, giving rise to the descending projections, although a part of axons pass through the parasubthalamic nucleus (PSTh; Bregma ~ −2.70 mm; injection 194/13; the same animals as in Figs. 1, 5, 11, and 13). Scale bar = 100 μm.

immunostaining for Parv (Fig. 1B) and GFP in Foxb1-Cre-GFP mice. In a few cases, the virus spread to astrocytes, but they fluoresced only very weakly (Fig. 3D,E). In some experiments, *Foxb1*-expressing cells of the mammillary nuclei were colabeled. The pathways emanating from these nuclei, namely, the mammillothalamic and the mammillotegmental tracts, were readily identified; so, too, were the corresponding terminal fields in the anterior thalamic nuclei (see Figs. 7D, 8A,B) and in the ventral and the dorsal tegmental nuclei (see Fig. 9). These specimens served as controls in the present study. Some of the Foxb1-immunopositive cells are known also to express Parv (Bilella et al., 2014). This finding was confirmed in the present study (see merged image in Fig. 1C,D). In 13 of the 16 injections, virtually all of the *Foxb1*-expressing neurons that are known to occur in the parvafox nucleus (Bilella et al., 2014) were infected with the virus (see Table 3). An example of this

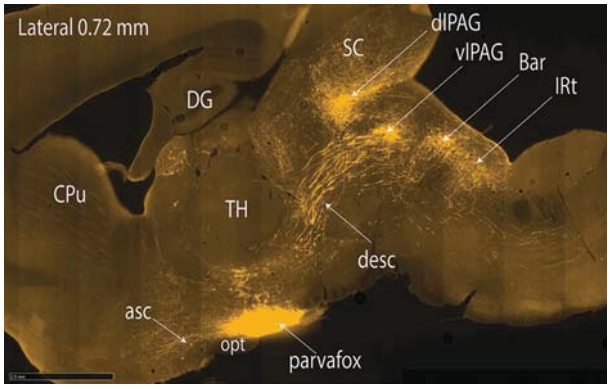

Figure 4. Axonal projections deriving from the Foxb1 neurons of the parvafox nucleus. Parasagittal sections of specimen 131-15. The injection site in the ventrolateral hypothalamus visualizes selectively the Foxb1-Cre-expressing neurons. From this Foxb1 aggregate of neurons, bundles of axons leave in various directions: ascending (asc), thalamic (TH), intrahypothalamic, and descending (desc). Various terminal fields, particularly those in the midbrain, are indicated.

can be seen in Figure 2, in which all of the neurons injected with the adenovirus AAV-tomato construct expressed the EGFP component (indicating the expression of *Foxb1*/Cre) as well.

Injection site

A representative injection site is shown in Figure 3. It depicts AAV-laden, *Foxb1*-expressing neurons and their interlacing dendrites. Together, these formed a dense, oval cluster with its long axis oriented parallel to the optic tract, running from Bregma –0.824 mm to Bregma –2.70 mm. The dendrites of the neurons were disposed in the coronal plane (clearly visible in Fig. 3B,C). Axons exited the labeled *Foxb1*-expressing neurons in various directions that have been described in detail by Nieuwenhuys as characteristic for the "hypothalamic aggression area" (Roeling et al., 1993, 1994a; see summary Fig. 16), namely, ascending (dorsal, lateral, and ventromedial), thalamic (dorsal and ventral), intrahypothalamic, and descending (dorsal, lateral, and medial).

Morphology of labeled axons

Morphologically, the axons exhibited varicosities, branches, and distinct terminal arborizations with patent "boutons terminaux," In the finest branches, the labeled axons displayed varicosities suggestive of synapses, the presence of which was confirmed by immunostaining for VGlut2 (Fig. 5). The density of the varicosities differed according to the area of passage. Indeed, many of the traversed brain areas could be innervated in this way.

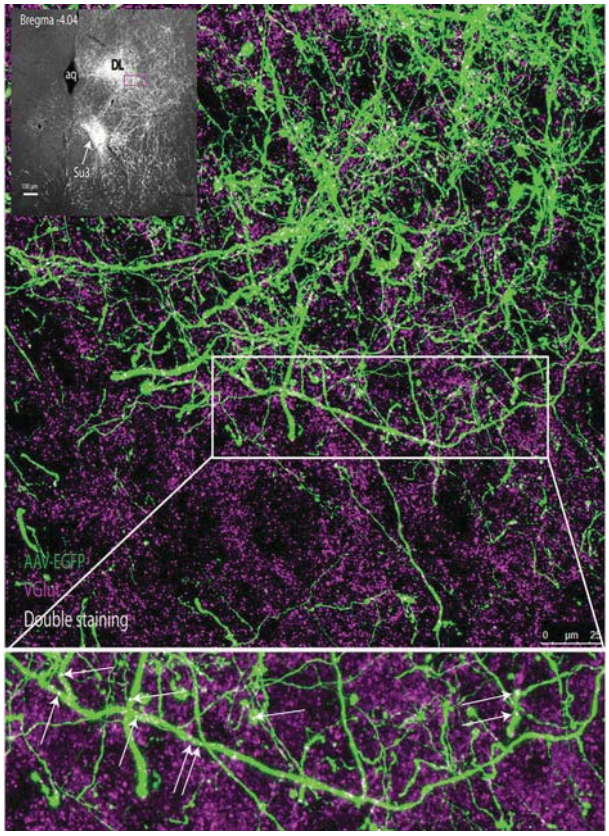

Figure 5. Confocal image illustrating the distribution of the vesicular glutamate transporter 2 (VGluT-2) in the glutamatergic, *Foxb1*-expressing terminals of the dorsolateral periaqueductal gray. The black and white inset indicates the region from which the image was taken. The lower **inset** depicts at higher magnification the small white spots within the immunopositive axonal endings (arrows). They are indicative of the merger of violet and green coloring and indirectly of the presence of the VGlut-2 transporter (Bregma –4.04 mm, injection 194/13). Scale bar = 25 μm.

Summary of results

The Foxb1-expressing neurons of the parvafox nucleus project to the telencephalon, diencephalon (thalamus and hypothalamus), midbrain, and hindbrain (Figs. 4, 6; see also summary Fig. 16). The strongest projection is to the periaqueductal gray (PAG), and the rest of the targets are sparsely labeled in comparison.

Ipsilateral vs. contralateral projections

The largest contingent of projections and terminals was observed ipsilaterally. However, in some regions, a contralateral mirror image of the terminals was seen (see below). The PAG and thalamic staining (e.g., the "virgolas"; see Fig. 8B) were exceptional in this respect, insofar as staining was observed only ipsilaterally. In what follows, we present the results systematically from rostral to caudal.

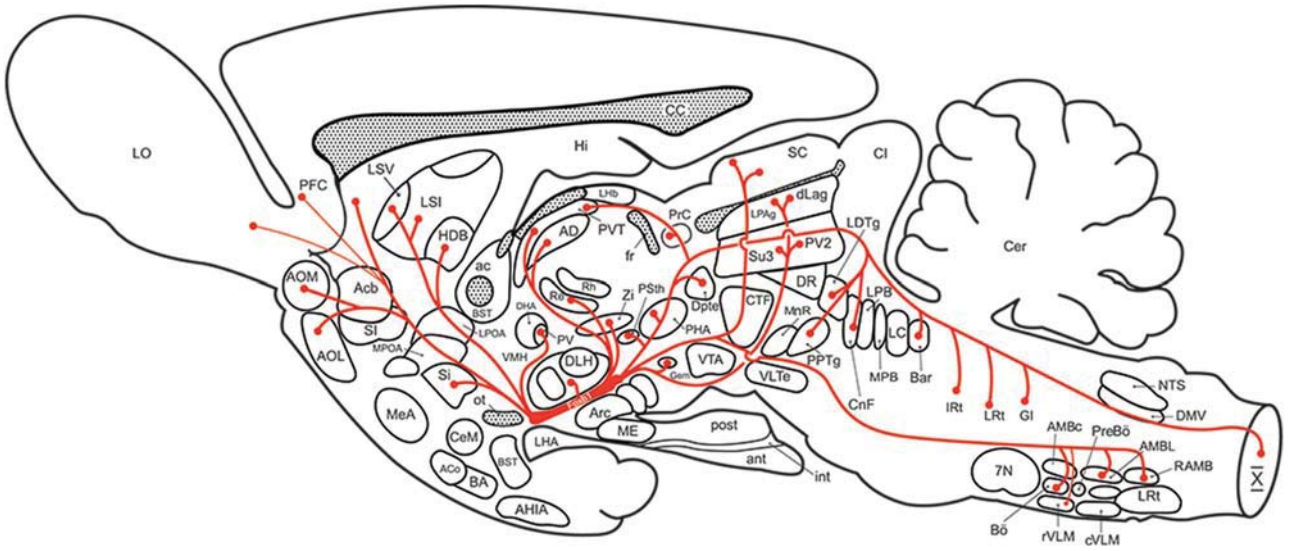

Figure 6. Schematic representation of a sagittal section of the mouse brain upon which the tracts leaving the Foxb1-expressing neurons in the lateral hypothalamus are projected (adapted from Roeling et al., 1993, 1994b). Three axonal tracts project rostrally, three distally, and two to the thalamus and hypothalamus. From these tracts, eight pathways are generated, which follow different courses and target different organs: 1) rostrodorsal, 2) rostrolateral, 3) rostromedial, 4) medial thalamic, 5) lateral thalamic, 6) distal dorsal, 7) laterodistal, and 8) mediodistal forebrain bundle. The anatomical organization of the ventral medulla is modified from the schematic drawing by Jänig (2006). The abbreviation listed here represent the structures that receive the terminals: AD, anterodorsal thalamic nucleus; AMBc, nucleus ambiguus, compact; AMBL, nucleus ambiguus, loose; AOL, anterior olfactory area, lateral part; AOM, anterior olfactory nucleus, medial; Bar, Barrington's nucleus; Bö, Bötzinger complex; CnF, cuneiform nucleus; dlPAG, dorsolateral periaqueductal gray; Gem, gemini hypothalamic nucleus; Gi, gigantocellular formation; HDB, nucleus of the horizontal limb of the diagonal band; IRt, intermediate reticular nucleus; LDTg, leterodorsal tegmental nucleus; lPAG, lateral periaqueductal gray; LRt, lateral reticular nucleus; LSI, lateral septal nucleus; LSV, lateral septal nucleus, ventral part; PFC, prefrontal cortex; PHA, posterior hypothalamic area; PPTg, posterior tegmental nucleus; PSTh, parasubthalamic nucleus; PV2, parvalbumin nucleus 2; PVT, paraventricular thalamic nucleus; RAMB, retroambiguus; Re, reuniens thalamic nucleus; rVLM, rostral ventrolateral medulla; SC, superior colliculus; Si, substantia innominata; Su3, suproculomotor nucleus; Zi, zona incerta.

Telencephalic projections

The ascending tract followed the mfb and consisted of a diffuse contingent of fine axons traversing the medial and the lateral preoptic area and, after reaching the diagonal band, proceeding to the ventral part of the lateral septal nucleus (Fig. 7). Rostrally, they ascended to the anterior amygdaloid nucleus, ran in the bed nucleus of the stria terminalis, and climbed to the lateral septum (Fig. 7). A few terminals were observed in the medial and lateral portions of the orbital cortex (Fig. 6), the olfactory nuclei (Fig. 6), and the olfactory bulb, lateral to the olfactory ventricle (see summary Fig. 16A, 16B).

Diencephalic projections

Stemming from the cells that were infected with the viral construct, the labeled axons passed into the mfb, ascended to the reuniens thalamic nuclei, and terminated in the dorsal thalamic nucleus (medial and lateral portions; Fig. 8; see also summary Fig. 16C,D,E,F). In the thalamic tract, considerable numbers of fibers run dorsal to the fornix to attain the paraventricular nucleus of the hypothalamus (Fig. 8C). Axons crossed the supraoptic decussation to reach the contralateral parvafox nucleus in the lateroventral hypothalamus. Contralaterally projecting axons were observed also in the supramammillary decussation.

Midbrain projections

Fibers from the parvafox nucleus coursing caudally went through the mfb, ran lateral to the mammillary bodies in the ventral tuberomammillary nucleus (VTM; Fig. 3K,L), traced a wide path through the ventral tegmental region, surrounded the fasciculus retroflexus, rose in dorsal direction in the posterior hypothalamus, and attained the PAG by passing through the medial zona incerta. Labeled axons reached the midbrain through three different pathways: 1) the dorsal (periventricular) fiber system, 2) the lateral (central tegmental) tract, and 3) the mfb.

Periventricular axons

The axons of the periventricular system formed thick bundles, which swept mediodorsally at premammillary levels in a periventricular location and then bent dorsocaudally, running alongside the lateral and ventral aspect of the central gray matter to the central tegmental field of the midbrain (Fig. 9).

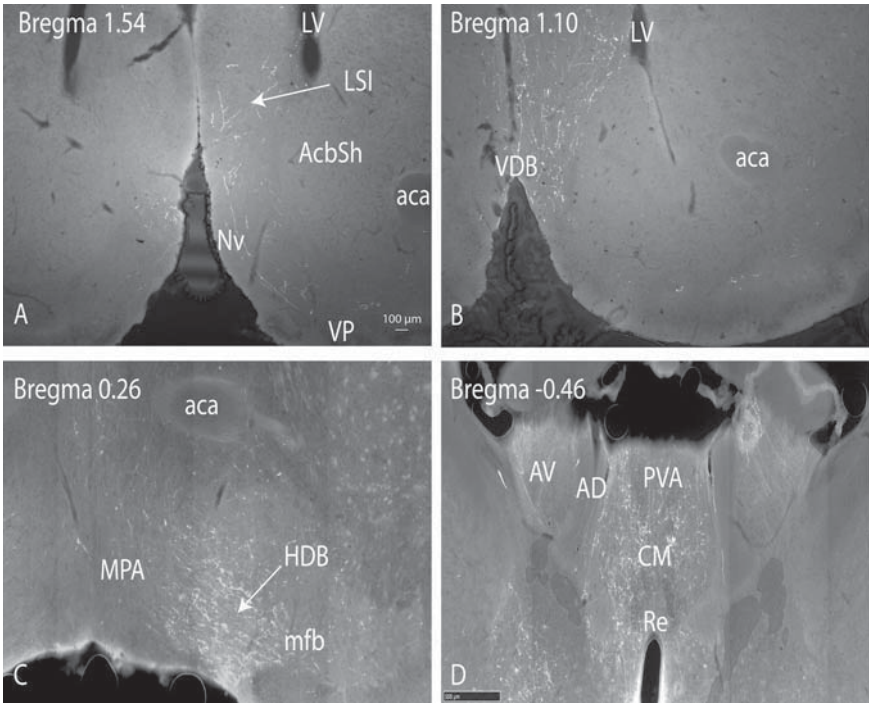

Figure 7. Coronal sections through the septum in a proximal (Bregma 1.54 mm; A) to distal (Bregma 0.62 mm; D) sequence. A low-density bundle of fibers from the parvafox nucleus passes through the navicular postolfactory nucleus (NV; **A**), the septal nuclei (A,B), and the nucleus of the vertical limb (**B**) headed for the frontal regions. **C:** High magnification of the region of the diagonal band, showing a rich collection of scattered axons and probable endings in this region. **D:** Projections in the thalamic region, in the anterior paraventricular thalamic nucleus (PVA), in the central medial thalamic nucleus (CM), and in the reuniens thalamic nucleus (Re; injection 249/13; the same animal as in Fig. 4). Scale bar = 100 µm in A (applies to A,B); 500 µm for C,D.

Central tegmental tract

The central tegmental tract conveyed axons that ran laterodorsally in the midbrain and innervated the deep gray and intermediate white layers of the superior colliculus (see Fig. 13) as well as the dorsolateral tegmental nucleus (Fig. 9).

mfb

The third major descending pathway is the mfb, which penetrates the ventral tegmental area. In the supramammillary decussation, some of the fibers switched to the contralateral side. From this region, axons coursed ventrodorsally in the midline and passed between the oculomotor region and the interstitial nucleus of Cajal into the ventromedial portion of the central gray matter to innervate the Su3 region. Some of the axons remaining in the mfb could be traced caudally in the pontine tegmentum and formed part of the ventromedial and the ventrolateral brainstem fiber system.

PAG projections

The *Foxb1*-expressing neurons projected mainly to five different areas that lay within or close to the PAG, namely, to a wedge-shaped region that encompassed the dorsolateral and the upper lateral columns (dL; L in Figs. 10A–G, 11), to a PAG-skirting column that lay ventral to the aqueduct (Su3 in Fig. 10D,E), to the deep mesencephalic nucleus (DpMe; Fig. 10E–G), to the cuneiform nucleus (CnF; Fig. 10H,I), and to the deep layers of the superior colliculus. At rostral levels of the PAG, the projections were largely restricted to a wedge-shaped segment that occupied the dorsolateral and the upper portions of its lateral columns (Figs. 10A–C, 11), mainly peripherally. This dense collection of terminal fields, of which the upper half was coincident with nNOS immunoreactivity (Fig. 11), extended from Bregma –2.80 mm rostrally to Bregma –5.00 mm distally (Fig. 10A–G) and was therefore the most prominent terminal field in the PAG (see also scheme in Fig. 12). At the midlevels of the PAG, both the dorsolateral/upper lateral columns and the Su3 were labeled (Fig. 10C–E), and the projection from the parvafox nucleus was distinctly bicolumnar. With the addition of the deep mesencephalic nucleus (DpMe; Fig. 10E–G), which lies outside the PAG, the projection became tri-columnar. At the other caudal levels of the PAG, the densest labeling coincided with the cluster of other Parv-

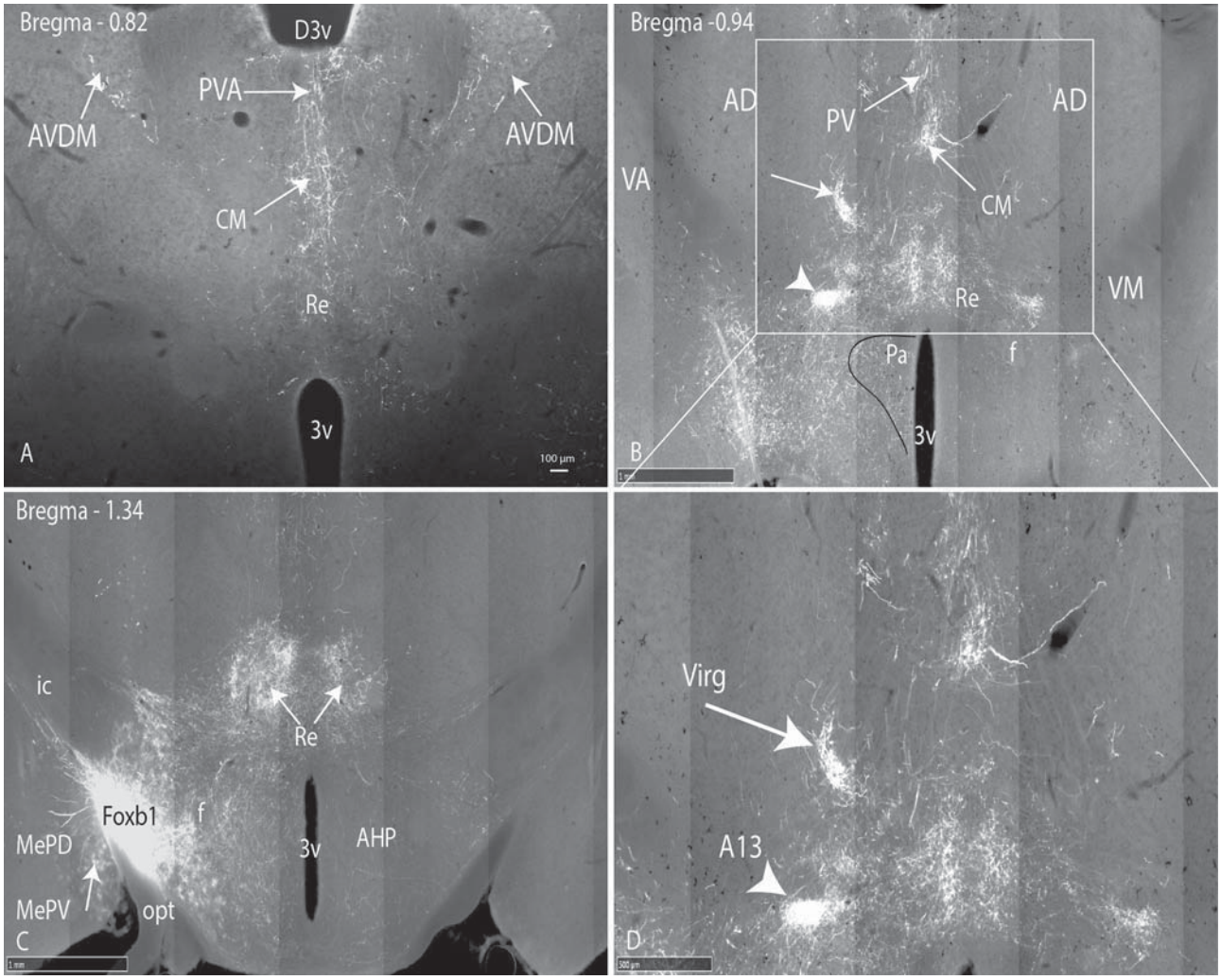

Figure 8. Epifluorescent images of coronal sections through the thalamus illustrating the projections thereto from the parvafox nucleus. **A:** At level Bregma –0.82 the axons from the *Foxb1*-expressing neurons project to the anterior paraventricular thalamic nucleus (PVA), the central medial thalamic nucleus (CM), and the reuniens thalamic nucleus (Re). The anterodorsal and anteroventral thalamic nuclei (AD, AVDM), receive a few terminals. **B:** Hypothalamic and thalamic projections (Bregma –0.94) are rich in the rostral part of the lateral hypothalamus. A dense, oval, ispilaterally stronger ending field is recognizable at the level of the zona incerta and may represent the A13 cell group (arrowhead). Slightly dorsally, a second, strictly ipsilateral, dense terminal field is probably restricted to the PC nucleus of the thalamus. We denote this small region as the "virgola field" because of its inverted comma shape (arrow; injection 249/13). **C:** Coronal section through thalamus and hypothalamus at level Bregma –1.34. The strong, overexposed labeling of the Foxb1 neurons in close proximity to the optic tract (ot) is readily recognizable. The rich terminal field in the reuniens nucleus is visible as well as axons passing through and terminals endings in the region of the zona incerta. The lateral hypothalamus is richly innervated by terminals deriving from Foxb1 axons whereas endings are rare or absent in the ventromedial hypothalamic nucleus. Note particularly the presence of endings in the lateral part of the periventricular nucleus of the hypothalamus. Axons pass also through the region of the cortical amygdala, in which some marked astrocytes also can be observed. **D:** Higher magnification of the thalamic labeling in B, with the two, aforementioned, strong and dense but spatially restricted terminal fields in the A13 region and in the "virgola field." Scale bar = 100 µm.

expressing neurons located in the LDTG, viz. in the so-called PV2 nucleus (Celio et al., 2013) and in the cuneiform nucleus (see also Fig. 10H,I).

The Foxb1 projections to the PAG reached their targets mainly ipsilaterally (Table 2), although in the Su3 a few contralateral ones were also seen (Fig. 10). The various terminal fields of the Foxb1 axons in the PAG are schematized in Figure 12 (and see also summary Fig. 16G,H). The projection to the PAG is glutamatergic, which was revealed by immunostaining for various neurotransmitter transporters (particularly VGlut2-positive ones; Fig. 5).

Hindbrain projections

A small number of axons forming part of the periventricular projection to the PAG went on caudally as part

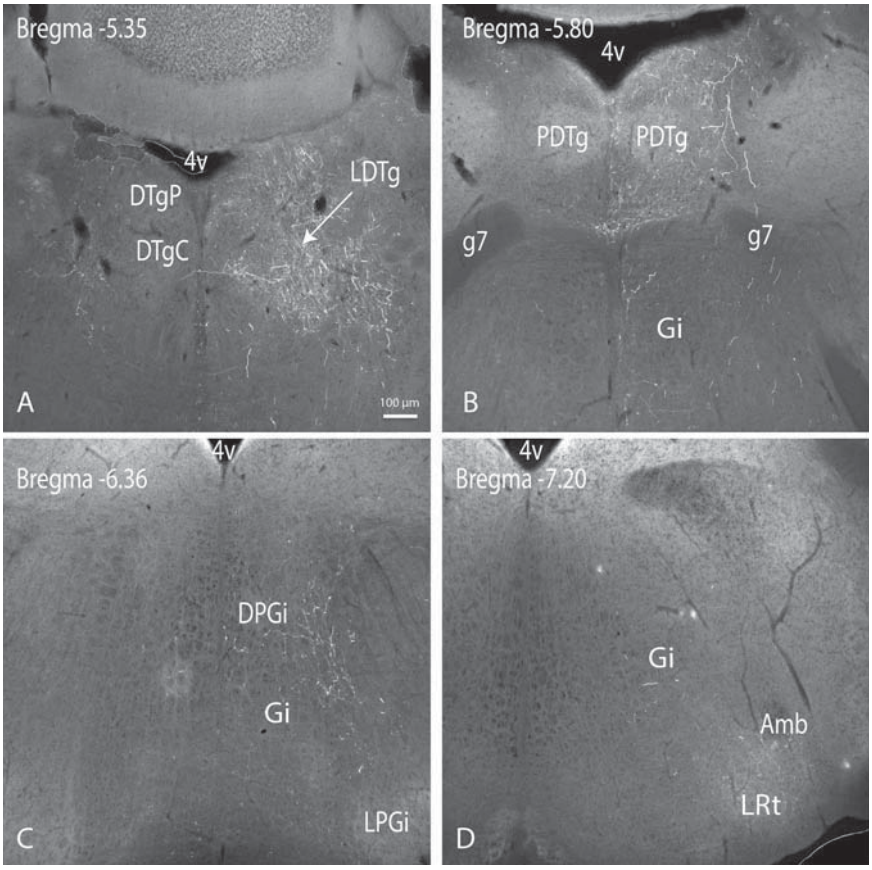

Figure 9. Epifluorescent images of coronal sections through the hindbrain, illustrating the projections thereto of axons emanating from the hypothalamic *Foxb1*-expressing neurons. The fibers traverse the dorsolateral tegmental nucleus (LDTg; Bregma ~ –5.35 mm; **A**), pass into the pons (Bregma ~ –5.80 mm; **B**), and continue their course through the dorsal paragigantocellular nucleus (DPGi; Bregma: ~ –6.36 mm; **C**). Projections are visible also in the gigantocellular reticular (Gi) and the lateral reticular (LRt) nuclei (**D**; injection 194/13). Scale bar = 100 µm.

of the dorsal brainstem fiber system. They terminated at three different hindbrain levels: 1) in the pontine tegmentum (including vestibular nuclei, laterodorsal tegmental nucleus, pedunculopontine nucleus, cuneiform nucleus, and Barrington's nucleus), 2) in the reticular substance (gigantocellular, intermediate, and lateral reticular nuclei), and 3) in the medulla oblongata Bötzinger complex, peri- and retroambigual regions; (see summary Fig. 14, 15, 16)).

Medulla oblongata

Some terminals ended in the retrofacial region of the ventrolateral medulla (Figs. 6, 14), in a region rich in vertically oriented TH-positive axons but devoid of TH-positive neurons, which may correspond to the Bötzinger complex, involved in the regulation of expiration (Fig. 14). The rostral ventrolateral medulla, a vasomotor center, also received terminal endings from the Foxb1-expressing neural population of the parvafox nucleus (Fig. 15A,A′,B,B′). At these levels the compact portion of the nucleus ambiguus was surrounded, particularly ventrally, by labeled axons and terminals, but none was observed within the boundaries of the nucleus. In the loose part of the ambiguous and in the retroambigual region, on the other hand, many axons terminated profusely in regions known to harbor neurons that control the cardiovascular system and the larynx (vocalization; Fig. 15C,C′)

Spinal projections

The Rexed layer X of the upper cervical segments received scattered terminals.

DISCUSSION

The parvafox nucleus projects widely

The projections of the subpopulation of *Foxb1*-expressing neurons in the lateral hypothalamic parvafox nucleus radiate in diverse directions. They extend rostrally to the olfactory bulbs, the orbitofrontal cortex,

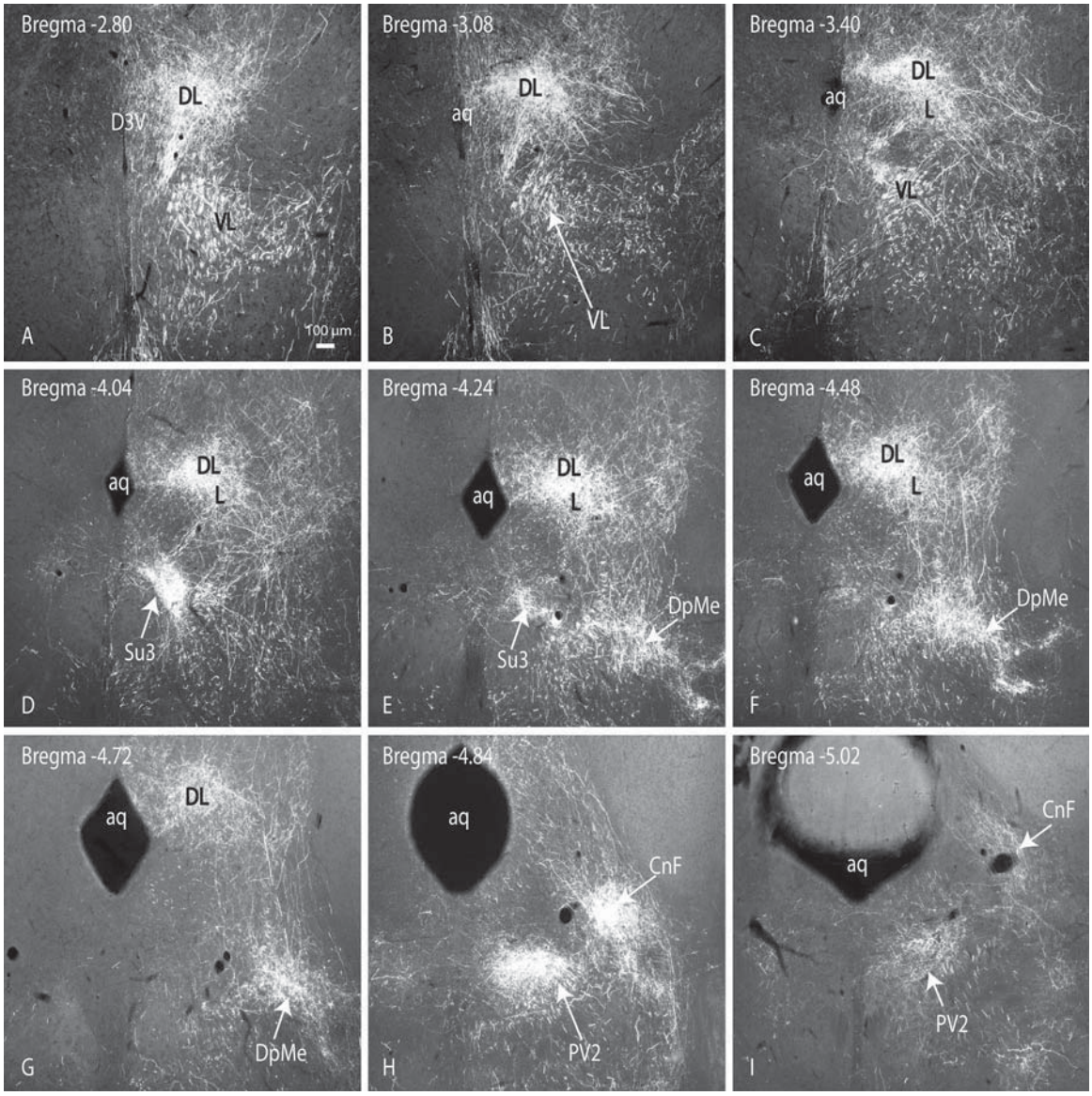

Figure 10. A–I: Epifluorescent images of nine consecutive coronal sections through the PAG, which was cut in a proximal (A)-to-distal (I) direction (E–G: Bregma ~ –4.20 mm to Bregma ~ –4.72 mm; H,I: Bregma ~ –5.00 mm). The images illustrate the projections of the lateral hypothalamic Foxb1-expressing neurons to the PAG. The coarse, AAV-EGFP-labeled axons radiate dorsally toward the rostral PAG and arborize in its dorsolateral (DL) and upper lateral portions (L), as well as in the deep layers of the superior colliculus (see Fig. 8). More caudally (D), the projections to the Su3 become visible. At Bregma ~ –4.04 mm (D), the axons separate into two bundles, which target the dorsolateral and the supraoculomotor (Su3) regions (E–G) and also populate the deep mesencephalic nucleus (DpMe). The terminal field in the dorsolateral region vanishes at level H and is replaced by one in the cuneiform nucleus (CnF; H,I). The ventrolateral terminal field is interrupted at levels F and G and reappears at level H, namely, in the PV2 nucleus (injection 194/13; the same animals as in Figs. 4, 11, and 12). Scale bar = 100 µm.

the septum, and the BNST; dorsally to the thalamus and the rostrolateral hypothalamus; and caudally to the superior colliculus, the PAG, the cuneiform nucleus, the pedunculopontine tegmental nucleus, the mesencephalic reticular formation, the gigantocellular nucleus, the retrofacial nucleus, and the retroambigual nucleus (Fig. 17). The extensive Foxb-expressing projections to many cell groups in the neural axis form the neural substrate for a variety of possible autonomic and behavioral functions. Compared with the projections of the Parv-immunopositive neurons in the parvafox nucleus (Celio et al., 2013), those of the Foxb1-expressing ones spread more widely.

Taking the findings of other investigators on the connections of the lateral hypothalamus as a whole (Berk and Finkelstein, 1982; Holstege, 1987; Hosoya and

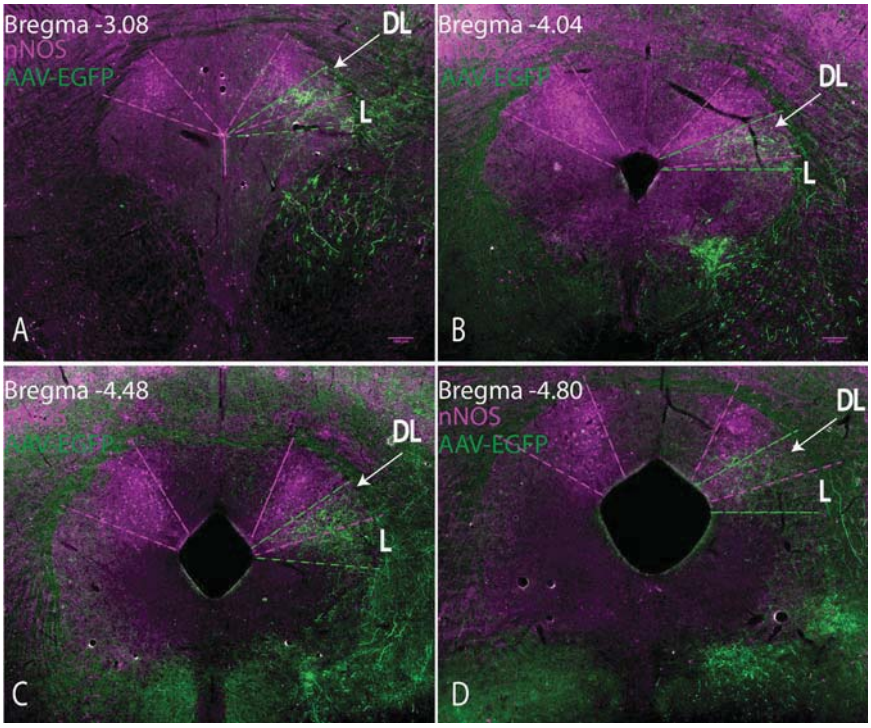

Figure 11. A–D: Epifluorescent images of four consecutive coronal sections through the PAG, which was cut in a proximal (A)-to-distal (D) direction (A,I: Bregma ∼ −3.08 mm to Bregma ∼ −4.80) of animal 25/16 injected in the parvafox of Foxb1-Cre mice stained for nNOS. The image illustrates the partial overlap of the projection from the lateral hypothalamic Foxb1-expressing neurons with neurons expressing the nitric oxide synthase (nNOS). The AAV-EGFP-labeled axons radiate dorsally toward the rostral PAG and arborize in its dorsolateral (DL) and upper lateral portions. The nNOS-positive neurons immunolabeled with a magenta fluorescent marker define the DLPAG. The magenta dashed lines indicate the approximate boundaries of the nNOS-positive cells, and the green dashed lines the boundaries of the terminal fields. The region included between the two lines in the middle corresponds to the region in which nNOS staining and the Foxb1-terminals coexist (injection 25/16). Scale bar = 100 μm.

Matsushita, 1981; Kita and Oomura, 1982; Saper et al., 1979; Veening et al., 1987; Villalobos and Ferssiwi, 1987a,b; Wolf and Sutin, 1966), the projections of the Foxb1-expressing cells are more confined. Most striking is the absence of projections to the amygdala, the parabrachial region, the locus coeruleus, the raphe nuclei, the dorsal vagus, and the solitary nucleus, which are the prominent target of other neuronal subfields in the lateral hypothalamus (Hahn and Swanson, 2010, 2012, 2015), even of the population of hypocretin/orexin (Peyron et al., 1998)- and melanin-concentrating hormone (MCH; Skofitsch et al., 1985)-positive neurons.

However, the output of the parvafox nucleus and of other regions of the lateral hypothalamus shares in common projections to the PAG. In all reports relating to the outputs of the lateral hypothalamus, the PAG is consistently one of the targets (Berk and Finkelstein, 1982; Hahn and Swanson, 2010, 2012, 2015; Holstege, 1987; Hosoya and Matsushita, 1981; Pelosi et al., 2006; Saper et al., 1979; Veening et al., 1987; Villalobos and Ferssiwi, 1987b).

The projection of the Foxb1-expressing neurons in the parvafox nucleus is special in that it extends to both the dorsolateral (dL) and the upper half of the lateral (L) PAG: it does not respect the boundaries known from the classical columns (Bandler et al., 2000). The dLPAG and LPAG are known to play a role in mediating the defensive responses to interoceptive stimuli (e.g., visceral pain) as well as to social and existential threats (e.g., confrontation with a predator and hypoxia; Bandler and Keay, 1996; Canteras and Graeff, 2014; Gross and Canteras, 2012). The responses involve a coordinated regulation of cardiovascular and respiratory activities (Bandler et al., 2000; Chaitoff et al., 2012; Dampney et al., 2013; Iigaya et al., 2010; Johnson et al., 2012). The dLPAG comprises partially overlapping subpopulations of NADPH/nNOS-, calbindin D28k (Barbaresi et al., 2013; Paxinos et al., 2009)- and calretinin-expressing neurons. This PAG column is also the most effective stimulation (or lesioning) site for the enhancement (or suppression) of lordotic behavior and is the target of a heavy contingent of descending inputs from

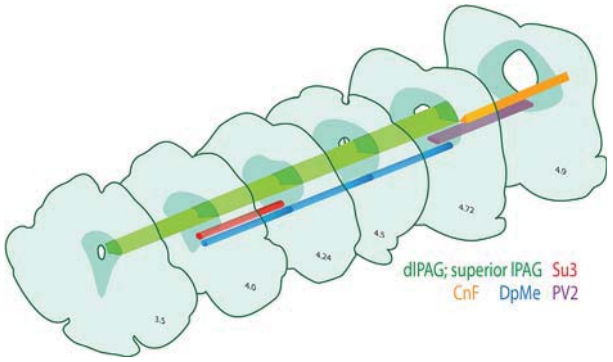

Figure 12. 3-D reconstruction of the terminal fields arising from the Foxb1-expressing neurons in the midbrain. The mouse PAG is represented in different rostrocaudal levels from Bregma –3.5 mm to Bregma –4.9 mm. In green is pictured the column of endings that reaches the dorsolateral (dlPAG) and the lateral periaqueductal gray (lPAG) from Bregma –3.5 mm to Bregma –4.72 mm. The red column shows the terminal fields to the supraoculomotor nucleus (Su3; Bregma –4.0 mm, Bregma –4.24 mm). The column of endings depicted in orange represents the terminals to the cuneiform nucleus (CnF; from Bregma –4.72 mm to –4.9 mm), the blue column the terminals at the level of the deep mesencephalic nucleus (DpMe), and the violet column the terminals on the PV2 (from Bregma –4.5 mm to –4.9 mm). Drawings modified from VanderHorst and Ulfhake (2006).

the hypothalamic ventromedial nucleus (Daniels et al., 1999). It also appears to harbor cells that are involved in vocalization (Larson, 1991). The lateral column of the PAG is also involved in predatory hunting and foraging behaviors (Comoli et al., 2003; Miranda-Paiva et al., 2003; Sukikara et al., 2006).

The LPAG sends projections to the lateral hypothalamus, especially at the tuberal levels, dorsolaterally to the fornix, in the region known to contain the MCH- and orexin-positive neurons (Bittencourt et al., 1992; de Lecea et al., 1998; Sakurai et al., 1998a). These two neural populations are involved in the control of locomotion (Krout et al., 2003) which is related to the food and water intake (De Parada et al., 2000). Therefore, on the basis of this physiological process, MCH and orexin are categorized as orexigenic neuropeptides (Qu et al., 1996; Sakurai et al., 1998a). However, the function of orexin and MCH is not limited to food intake. Orexin is also involved in arousal and foraging (Chemelli et al., 1999; Hara et al., 2001; Nishino et al., 2000): activation of the orexin-expressing neurons increases the probability of transition from sleep to wakefulness (Adamantidis et al., 2007).

The Su3 region is the only target that the Foxb1-expressing and Parv-immunopositive neurons (Celio et al., 2013) in the parvafox nucleus share in common.

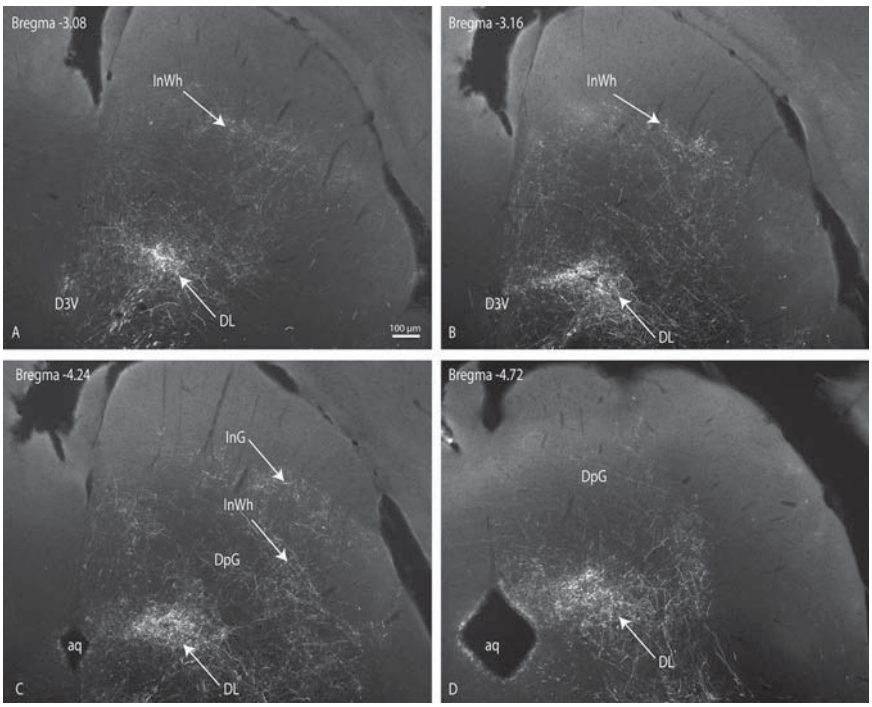

Figure 13. Epifluorescent images of coronal sections through the superior colliculus in a proximal (Bregma ~ –3.08 mm; A) to distal (Bregma ~ –4.72 mm; D) direction. A conspicuous bundle of fibers arborizes in the intermediate white layer (InWh). **A,B:** Proceeding caudally, at Bregma level ~ –4. 24 mm, the fibers reach the intermediate layer of the superior colliculus (InG), the InWh, and the deep layer of the superior colliculus (DpG; **C,D**; injection 194/13; the same animals as in Figs. 1, 3, 5, and 11). Scale bar = 100 µm.

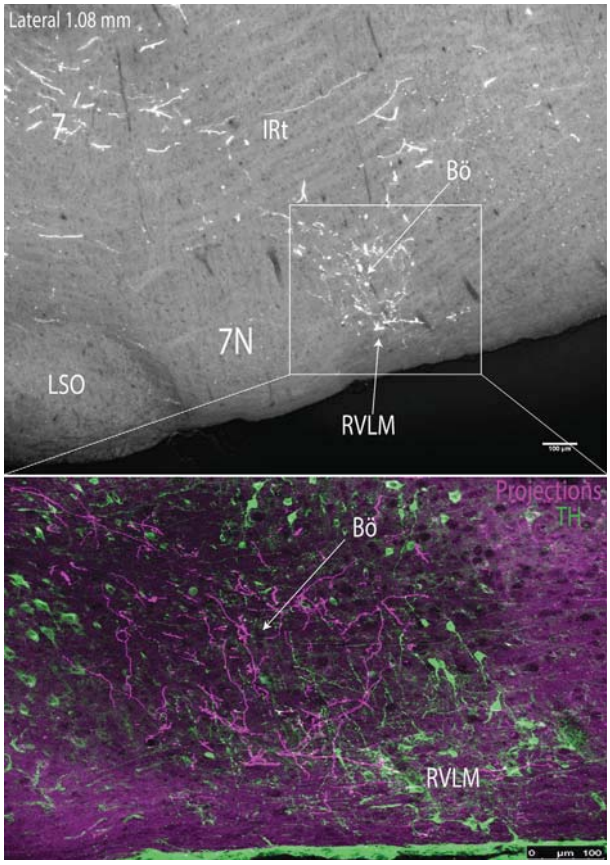

Figure 14. Epifluorescent image of parasagittal section trough the hindbrain (lateral 1.08 mm). The image illustrates the projections of the lateral hypothalamic Foxb1-expressining neurons to the rostral ventrolateral medulla. The **inset** shows an enlarged image of the projections (magenta) probably innervating the Bötzinger complex. In green the tyrosine hydroxylase-positive neurons are shown. Confocal image (injection 131/15). Scale bar = 100 µm.

No other recent publications relating to the hypothalamus report projections in the Su3, not even after stereotactic injections into targeted areas that lie slightly more medial to the parvafox nucleus, such as the hypothalamic tuberal nucleus (Canteras, 1992), the subfornical region (Goto et al., 2005) and the juxtaventromedial portion of the lateral hypothalamus (Hahn and Swanson, 2010, 2012, 2015). In the classical study conducted by Berk and Finkelstein (1982), which involved autoradiographic tracing with ^{3}H-leucine, terminals in a region that lay close to the Su3 were documented (injection M15) but were not commented on as being in any way noteworthy.

The Su3 receives inputs from the linear nucleus of the ventral tegmental region (Del-Fava et al., 2007), the intergeniculate leaflet (Morin and Blanchard, 2005), various oculomotor-related sites (Buttner-Ennever et al., 2002), and the deep cerebellar nuclei (Gonzalo-Ruiz et al., 1990). A subpopulation of Su3 neurons (Van Bockstaele and Aston-Jones, 1992) projects to the rostral ventrolateral medulla (RVLM), a region that controls cardiovascular activity (Van Bockstaele et al., 1989, 1991) and to the nucleus ambiguus (Ennis et al., 1997). The neurons of the Su3 are activated when a predator is confronted and during hunting (Comoli et al., 2003).

The context-avoidance behavior of freezing rats and their response to predator-associated odors are accompanied by a marked elevation of the expression levels of c-Fos in the cuneiform nucleus (Allen et al., 1996; Carrive et al., 1997; Dielenberg et al., 2001b; Walker and Winn, 2007), which also plays a role in the cardiovascular and respiratory changes associated with defensive reactions (e.g., increases in heart rate and in blood pressure; Korte et al., 1992; Netzer et al., 2011). The cuneiform nucleus receives inputs from the anterior hypothalamic area and the dorsal premammillary nucleus (Motta et al., 2009) as well as from the lateral hypothalamic LHAjvd and LHAjvv (Hahn and Swanson, 2015), although those from the latter two regions are more scarce than those from the Foxb1-expressing neurons of the parvafox nucleus (Bernard et al., 1989; Netzer et al., 2011).

The superior colliculus is a laminated midbrain structure that acts to organize gaze movements, playing a role in orientation movements of the head and the eye in response to various stimuli (Dean et al., 1989). The superficial layers receive retinal information (May, 2006), and the deeper layers receive and integrate information from numerous sensory modalities (Drager and Hubel, 1975; May, 2006; McHaffie et al., 1989; Stein et al., 2009). The presence of a predator is registered in the lower visual field, outputs from which activate the medial deep layer of the superior colliculus, thereby triggering a signal-avoidance response. Appetitive stimuli are detected in the upper visual field, outputs from which activate the lateral deep layers of the superior colliculus (Comoli et al., 2012), whereby a signal-approach reaction is triggered (e.g., predatory hunting; Furigo et al., 2010). The lateral superior colliculus plays a role in the circuitry for sense-guided orientation decisions (Boehnke and Munoz, 2008; Dean et al., 1989; Felsen and Mainen, 2008) and integrates relevant sensory information for prey detection (Boehnke and Munoz, 2008).

The superior colliculus receives information from the ventromedial hypothalamic nucleus (VMH), the dlPAG, the vlPAG (Furigo et al., 2010; Mantyh, 1982; Wiberg, 1992), and the premammillary nucleus (PMV; Canteras and Swanson, 1992). It projects directly to the dlPAG (Rhoades et al., 1989) and, via this route, to the

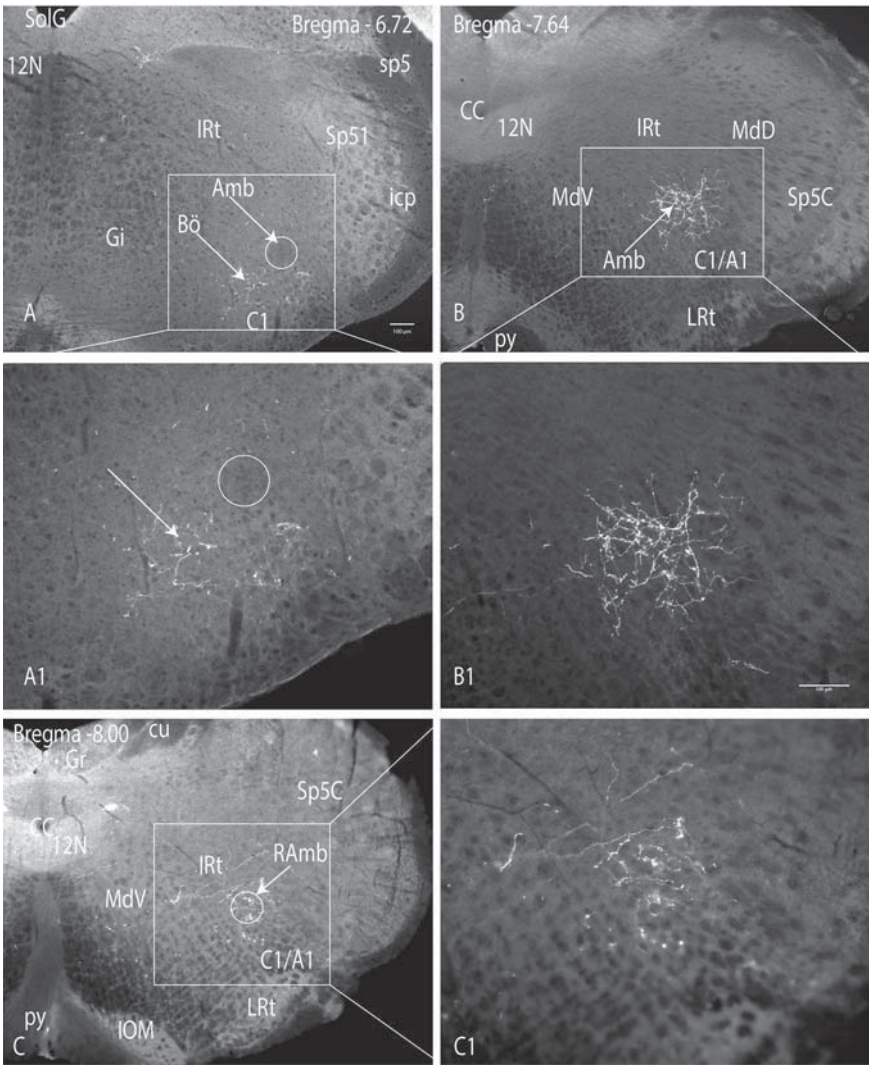

Figure 15. Epifluorescent images of a coronal section through the hindbrain. **A:** In the medulla oblongata, sparse tomato-positive fibers and terminals occupy a region ventral to the ambiguus nucleus (Amb), corresponding to the Bötzinger (Bö) complex (Bregma –6.72 mm). **A1:** Higher magnification the immunopositive axonal endings (arrows) in the Bö region. **B:** More caudally, the axons arising from the Foxb1-expressing neurons of the parvafox nucleus reach the region of the loose ambiguus (Bregma –7.64 mm). **B1:** Higher magnification of the rich ramification of immunopositive axonal endings in this region. **C:** At level Bregma –8.00, endings are found in the retroambigual region. **C1:** Higher magnification of the cluster of endings encircled in C. Scale bar = 100 μm.

cuneiform nucleus (Redgrave et al., 1988). The dlPAG and adjacent portions of the superior colliculus may thus form a part of a defense mechanism in the midbrain. The superior colliculus projects also to the lPAG (Furigo et al., 2010), which seems to be a nodal part of the circuitry involved in the decision-making process between different behavioral responses such as hunting or foraging (Sukikara et al., 2006).

Taken together, these data support the "sentinel hypothesis" (Merker, 1980) cited by R. Rieck et al. (1986). This postulate suggests that the superior colliculus, in particular, the medial deep layer, could function as a sentinel for dangerous stimuli and be involved in the behavioral responses that comprise the strategies of defense in a threatening situation (Carvalho-Netto et al., 2006; Dean et al., 1988), whereas the lateral deep layer controls orientation of pursuit-like movements and influences arousal, motivation, motor learning planning, and motor output which are critical for foraging and hunting behaviors (Furigo et al., 2010).

Other projections that may be implicated in defensive mechanism

Projections to the vestibular nuclei

The vestibular nuclei are involved in the control and regulation of blood pressure during movement and

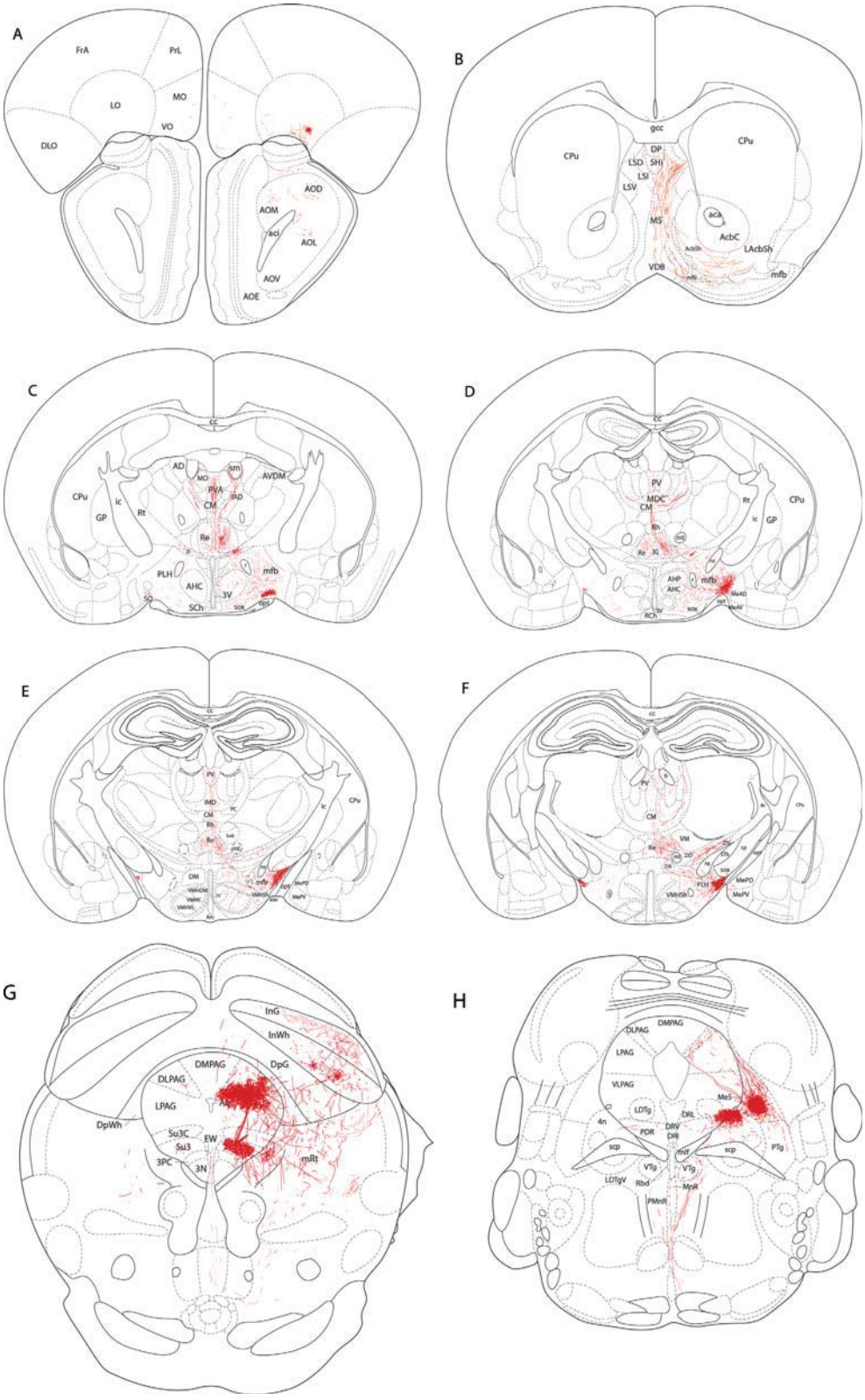

Figure 16. **I–H:** Series of coronal drawings at 8 hindbrain levels of the mouse brain in which the projections of the hypothalamic Foxb1 neurons are represented. The source of all these projections the virus-infected Foxb1 neurons seen in drawings D–F. The main targets in the dorsolateral and upper lateral PAG, as well as the Su3 and PV2 nuclei, are depicted in G and H. Note the absence of terminals in the amygdala, parabrachial nuclei, and solitary tract. Drawings modified from Franklin and Paxinos (2008).

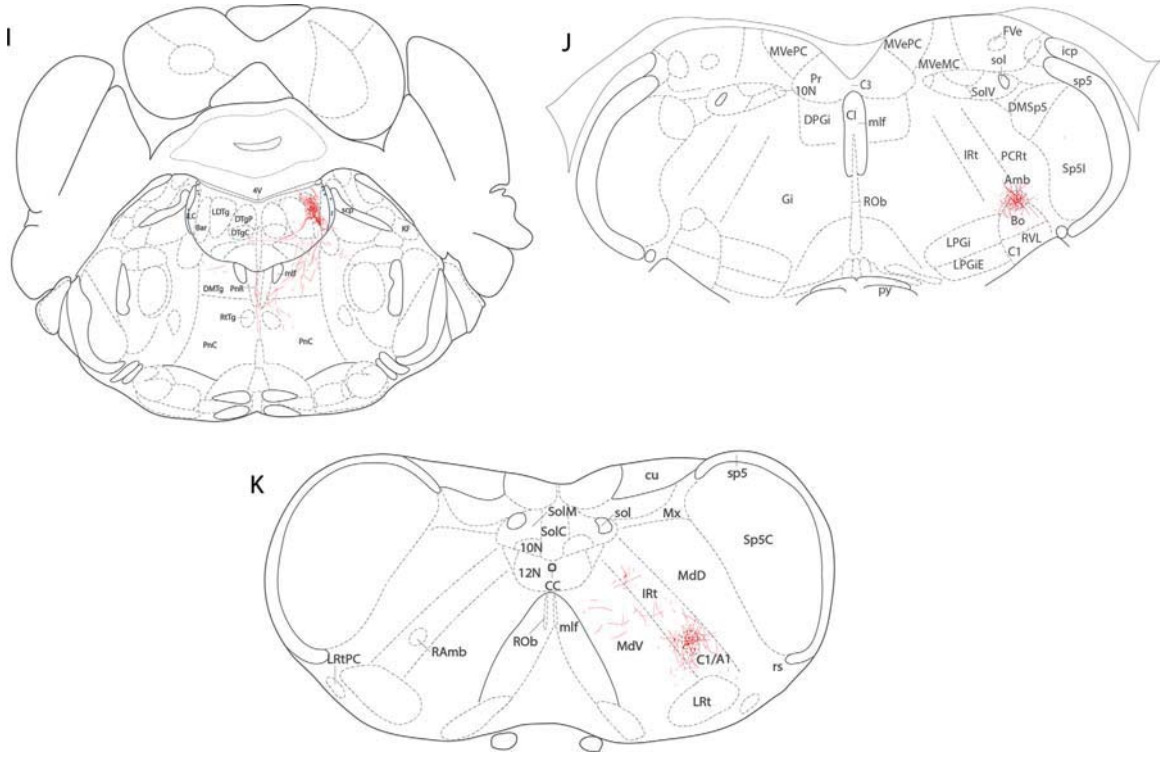

Figure 16. **A–K:** Series of coronal drawings at 10 levels of the mouse brain in which the projections of the hypothalamic Foxb1 neurons are represented. Drawings modified from Franklin and Paxinos (2008).

changes in posture via their influence on the sympathetic nervous system (Tang and Gernandt, 1969). Outputs from the cervical spinal tract project to the autonomic region of the vestibular nuclei. The reticular formation, including the lateral reticular nucleus (LRt), projects directly to the vestibular nuclei (Jian et al., 2005) and receives inputs from visceral and somatosensory receptors (Ammons, 1987; Blair, 1987; Drew et al., 1996; Fields et al., 1977; Peterson et al., 1976; Schulz et al., 1983; Thies, 1985; Yates and Stocker, 1998) as well as from the raphe nucleus (Blair and Evans, 1991; Knuepfer and Holt, 1991; Lumb and Morrison, 1984), whereby visceral and somatosensory information is integrated.

Projections to the gigantocellular and the lateral reticular nuclei

The gigantocellular reticular formation plays an important role in behavioral arousal (Boissard et al., 2002; Morest, 1961; Morest and Sutin, 1961; Steriade et al., 1984) as well as in the modulation of pain (Mason, 2005; Nagata et al., 2003) and motor activity (Fay and Norgren, 1997; Hattox et al., 2002; Robinson et al., 1994). It receives projections from diverse sources, including the nucleus of the solitary tract, the preoculomotor nucleus, the Su3, the PAG, the lateral hypothalamus, the periventricular nucleus, and the medial prefrontal cortex (Van Bockstaele et al., 1989). The main targets of the gigantocellular nucleus are the locus coeruleus and the spinal cord (from the gigantocellualr reticular formation; Hermann et al., 2003; Holstege and Kuypers, 1982; Liang et al., 2013).

The LRt is a precerebellar agglomeration of mossy fibers, which relays information to the cerebellar cortex. It receives a massive contingent of afferents from the spinal cord (Brodal, 1949; Kunzle, 1973; Morin et al., 1966) as well as descending fibers from the cerebral cortex (Brodal et al., 1967; Kunzle and Wiesendanger, 1974), the red nucleus (Mizuno et al., 1973), and the superior colliculus (Mizuno et al., 1973). The lateral reticular formation projects a massive bundle of fibers to the cerebellum, which processes the inputs it receives from the different areas. Consequently, only filtered information appertaining to control of movements is delivered to the cerebellum (Alstermark and Ekerot, 2013).

Projections to the olfactory bulb

Common stimuli that trigger specific behavioral responses are the presence of a predator or prey. In both instances, sentience of the presence is registered

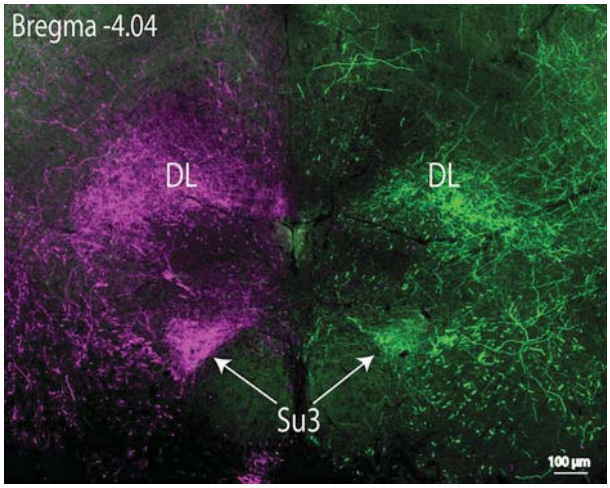

Figure 17. Epifluorescent image of projections in the PAG at Bregma level –4.04 mm after a bilateral injection of two different viral tracers, one bearing dTomato and the other EGFP in the parvafox nucleus. The projections are symmetrical (injection 9/15). Scale bar = 100 µm.

in the visual or the olfactory system. An odor is detected by the olfactory system, from which a bundle of fibers runs consecutively to the amygdala, the ventromedial hypothalamic nucleus (VMH), the lateral hypothalamus and the dlPAG, which together form a specific circuitry (Canteras, 2002; Dielenberg et al., 2001b; Motta et al., 2009).

Projections to the prefrontal cortex

The prefrontal cortex mediates the autonomic responses to emotional situations. Its projections to the central nervous system influence cognitive processes and decision making. It is implicated in the control of hearth rate, blood pressure, respiration, and gastric motility (Diorio et al., 1993; Feldman and Conforti, 1985; Gabbott et al., 2005; Van Eden and Buijs, 2000). The prefrontal cortex plays a pivotal role in mediating the interactions between the central and the autonomic nervous systems. The ventromedial portion projects to the hypothalamus (PVN, DMH, LH) and the dorsomedial one directly to the autonomic centers in the brainstem and spinal cord. The former portion projects to the vlPAG and the latter to the dlPAG (Van Eden and Buijs, 2000).

Projections to the lateral septum

The lateral septum is a sexually dimorphic nucleus, which is the target of vasopressin-expressing innervations. It is heavily interconnected with sites in the lateral hypothalamus that are implicated in the control of rewarding, stimulus-driven states (de Vries et al., 1981). It is also involved in coping with stress (Koolhaas et al., 1998) as well as in regulating social behavior and anxiety (Veenema and Neumann, 2008). Activation of the CRF2 receptor-expressing subpopulation of neurons in the lateral septum generates anxiety (Anthony et al., 2014).

Projections to the midline nuclei of the thalamus

The thalamic midline nuclei (PV, PVA, CM, IAM, and Rh) harbor neurons that project to the nucleus accumbens, the medial frontal cortex, and the amygdala (Bubser and Deutch, 1998; Otake and Nakamura, 1998; Su and Bentivoglio, 1990); they are involved in viscerolimbic functions and in the self-perception of viscerosensory stimuli (Cassel et al., 2013; Otake and Nakamura, 1998; Van der Werf et al., 2002).

Comparison of our findings with existing data on the defensive responses

The independent, multiple circuits that process the different types of defensive reaction involve the medial, but not the lateral, hypothalamus (Gross and Canteras, 2012; Jordan, 1990). In the classical work by Ranson's group, the defense responses was localized lateral to the fornix (Kabat et al., 1935), whereas the observation of Hess and his school (Akert, 1981; Fernandez De Molina and Hunsperger, 1962; Hess and Brügger, 1943; Hunsperger, 1956) implicated the perifornical and pericommissural (Gansser) regions, a finding that has since been confirmed in several studies (Nakao, 1958; Wasman and Flynn, 1962). The defensive response to the presence of a predator involves the dorsal premammillary nucleus (Canteras, 2002). Recent optogenetic work in mice has localized the center of an intermale attack to the ventrolateral subdivision of the ventromedial nucleus (Lin et al., 2011) and a stalking one to the lateral portion (Wasman and Flynn, 1962).

A participation of this most recondite portion of the lateral hypothalamus, which harbors the Foxb1-expressing neurons, in the stereotyped behavioral aspects of a defensive response has never been reported. Electrical stimulation of this zone in the cat (Hess, 1947, 1957; Karplus and Kreidl, 1910; Ranson and Magoun, 1933) leads to changes in cardiovascular, respiratory, and pupillary activity as well as to salivation, micturition, and defecation. The cardiovascular effects have been confirmed by the microinjection of L-glutamate, which activates neurons but not the axons of passage (Allen and Cechetto, 1992; Spencer et al., 1989). It may therefore be deduced that the parvafox nucleus is concerned not with the behavioral but with

the autonomic manifestations of the defense response. It is to be expected that electrode recording or chemo- and optogenetic techniques will help to establish the role played by this nucleus in various threatening, stressful, and other emotional situations.

ACKNOWLEDGMENTS

We thank Dr. Alexander Babalian for instructing A.B. in the technique of stereotactic intracerebral injection, Dr. Franck Girard for his help in genotyping, and Simone Eichenberger for her help in the handling of the mice. The technical assistance of Christiane Marti and Laurence Clément is also gratefully acknowledged.

CONFLICT OF INTEREST STATEMENT

The authors declare that they have no conflicts of interest.

ROLE OF AUTHORS

All authors had full access to the data in the study and take responsibility for its integrity and the accuracy of the analysis. MRC designed and oversaw the project. GA-B supplied the Foxb1 mice; AB made the stereotactic injections, prepared the sections and performed immunohistochemistry. AB and MRC took pictures, evaluated the results, and together with GA-B wrote the manuscript.

LITERATURE CITED

Adamantidis AR, Zhang F, Aravanis AM, Deisseroth K, de Lecea L. 2007. Neural substrates of awakening probed with optogenetic control of hypocretin neurons. Nature 450:420–424.

Akert K, editor. 1981. Biological order and brain organiization: selected works of W.R. Hess. Berlin: Springer-Verlag.

Allen GV, Cechetto DF. 1992. Functional and anatomical organization of cardiovascular pressor and depressor sites in the lateral hypothalamic area: I. Descending projections. J Comp Neurol 315:313–332.

Allen LF, Inglis WL, Winn P. 1996. Is the cuneiform nucleus a critical component of the mesencephalic locomotor region? An examination of the effects of excitotoxic lesions of the cuneiform nucleus on spontaneous and nucleus accumbens induced locomotion. Brain Res Bull 41:201–210.

Alstermark B, Ekerot CF. 2013. The lateral reticular nucleus: a precerebellar centre providing the cerebellum with overview and integration of motor functions at systems level. A new hypothesis. J Physiol 591:5453–5458.

Alvarez-Bolado G, Celio MR. 2015. The ventrolateral hypothalamic area and the parvafox nucleus: role in the expression of (positive) emotions? J Comp Neurol 524: 1616–1623.

Alvarez-Bolado G, Zhou X, Cecconi F, Gruss P. 2000a. Expression of Foxb1 reveals two strategies for the formation of nuclei in the developing ventral diencephalon. Dev Neurosci 22:197–206.

Alvarez-Bolado G, Zhou X, Voss AK, Thomas T, Gruss P. 2000b. Winged helix transcription factor Foxb1 is essential for access of mammillothalamic axons to the thalamus. Development 127:1029–1038.

Ammons WS. 1987. Characteristics of spinoreticular and spinothalamic neurons with renal input. J Neurophysiol 58: 480–495.

Anthony TE, Dee N, Bernard A, Lerchner W, Heintz N, Anderson DJ. 2014. Control of stress-induced persistent anxiety by an extra-amygdala septohypothalamic circuit. Cell 156:522–536.

Bandler R, Keay KA. 1996. Columnar organization in the midbrain periaqueductal gray and the integration of emotional expression. Prog Brain Res 107:285–300.

Bandler R, Keay KA, Floyd N, Price J. 2000. Central circuits mediating patterned autonomic activity during active vs. passive emotional coping. Brain Res Bull 53:95–104.

Barbaresi P, Mensa E, Lariccia V, Pugnaloni A, Amoroso S, Fabri M. 2013. Differential distribution of parvalbumin- and calbindin-D28K-immunoreactive neurons in the rat periaqueductal gray matter and their colocalization with enzymes producing nitric oxide. Brain Res Bull 99:48–62.

Barson JR, Morganstern I, Leibowitz SF. 2013. Complementary roles of orexin and melanin-concentrating hormone in feeding behavior. Int J Endocrinol 2013:983964.

Berk ML, Finkelstein JA. 1982. Efferent connections of the lateral hypothalamic area of the rat: an autoradiographic investigation. Brain Res Bull 8:511–526.

Bernard JF, Peschanski M, Besson JM. 1989. Afferents and efferents of the rat cuneiformis nucleus: an anatomical study with reference to pain transmission. Brain Res 490:181–185.

Bilella A, Alvarez-Bolado G, Celio MR. 2014. Coaxiality of Foxb1- and parvalbumin-expressing neurons in the lateral hypothalamic PV1 nucleus. Neurosci Lett 566:111–114.

Bittencourt JC, Presse F, Arias C, Peto C, Vaughan J, Nahon JL, Vale W, Sawchenko PE. 1992. The melanin-concentrating hormone system of the rat brain: an immuno- and hybridization histochemical characterization. J Comp Neurol 319:218–245.

Blair RW. 1987. Responses of feline medial medullary reticulospinal neurons to cardiac input. J Neurophysiol 58:1149–1167.

Blair RW, Evans AR. 1991. Responses of medullary raphespinal neurons to electrical stimulation of thoracic sympathetic afferents, vagal afferents, and to other sensory inputs in cats. J Neurophysiol 66:2084–2094.

Boehnke SE, Munoz DP. 2008. On the importance of the transient visual response in the superior colliculus. Curr Opin Neurobiol 18:544–551.

Boissard R, Gervasoni D, Schmidt MH, Barbagli B, Fort P, Luppi PH. 2002. The rat pontomedullary network responsible for paradoxical sleep onset and maintenance: a combined microinjection and functional neuroanatomical study. Eur J Neurosci 16:1959–1973.

Brodal A. 1949. Spinal afferents to the lateral reticular nucleus of the medulla oblongata in the cat; an experimental study. J Comp Neurol 91:259–295, incl. 252 plates.

Brodal P, Marsala J, Brodal A. 1967. The cerebral cortical projection to the lateral reticular nucleus in the cat, with special reference to the sensorimotor cortical areas. Brain Res 6:252–274.

Bubser M, Deutch AY. 1998. Thalamic paraventricular nucleus neurons collateralize to innervate the prefrontal cortex and nucleus accumbens. Brain Res 787:304–310.

Buttner-Ennever JA, Horn AK, Graf W, Ugolini G. 2002. Modern concepts of brainstem anatomy: from extraocular motoneurons to proprioceptive pathways. Ann N Y Acad Sci 956:75–84.

Canteras NS. 2002. The medial hypothalamic defensive system: hodological organization and functional implications. Pharmacol Biochem Behav 71:481–491.

Canteras NS, Graeff FG. 2014. Executive and modulatory neural circuits of defensive reactions: implications for panic disorder. Neurosci Biobehav Rev 46:352–364.
Canteras NS, Swanson LW. 1992. The dorsal premammillary nucleus: an unusual component of the mammillary body. Proc Natl Acad Sci U S A 89:10089–10093.
Carrive P, Leung P, Harris J, Paxinos G. 1997. Conditioned fear to context is associated with increased Fos expression in the caudal ventrolateral region of the midbrain periaqueductal gray. Neuroscience 78:165–177.
Carvalho-Netto EF, Markham C, Blanchard DC, Nunes-de-Souza RL, Blanchard RJ. 2006. Physical environment modulates the behavioral responses induced by chemical stimulation of dorsal periaqueductal gray in mice. Pharmacol Biochem Behav 85:140–147.
Cassel JC, Pereira de Vasconcelos A, Loureiro M, Cholvin T, Dalrymple-Alford JC, Vertes RP. 2013. The reuniens and rhomboid nuclei: neuroanatomy, electrophysiological characteristics and behavioral implications. Prog Neurobiol 111:34–52.
Celio MR. 1990. Calbindin D-28k and parvalbumin in the rat nervous system. Neuroscience 35:375–475.
Celio MR, Babalian A, Ha QH, Eichenberger S, Clement L, Marti C, Saper CB. 2013. Efferent connections of the parvalbumin-positive (PV1) nucleus in the lateral hypothalamus of rodents. J Comp Neurol 521:3133–3153.
Chaitoff KA, Toner F, Tedesco A, Maher TJ, Ally A. 2012. Effects of inducible nitric oxide synthase blockade within the periaqueductal gray on cardiovascular responses during mechanical, heat, and cold nociception. Neurol Sci 33:69–78.
Chemelli RM, Willie JT, Sinton CM, Elmquist JK, Scammell T, Lee C, Richardson JA, Williams SC, Xiong Y, Kisanuki Y, Fitch TE, Nakazato M, Hammer RE, Saper CB, Yanagisawa M. 1999. Narcolepsy in orexin knockout mice: molecular genetics of sleep regulation. Cell 98:437–451.
Comoli E, Ribeiro-Barbosa ER, Canteras NS. 2003. Predatory hunting and exposure to a live predator induce opposite patterns of Fos immunoreactivity in the PAG. Behav Brain Res 138:17–28.
Comoli E, Das Neves Favaro P, Vautrelle N, Leriche M, Overton PG, Redgrave P. 2012. Segregated anatomical input to sub-regions of the rodent superior colliculus associated with approach and defense. Front Neuroanat 6:9.
Dampney RA, Furlong TM, Horiuchi J, Iigaya K. 2013. Role of dorsolateral periaqueductal grey in the coordinated regulation of cardiovascular and respiratory function. Auton Neurosci 175:17–25.
Daniels D, Miselis RR, Flanagan-Cato LM. 1999. Central neuronal circuit innervating the lordosis-producing muscles defined by transneuronal transport of pseudorabies virus. J Neurosci 19:2823–2833.
de Lecea L, Kilduff TS, Peyron C, Gao X, Foye PE, Danielson PE, Fukuhara C, Battenberg EL, Gautvik VT, Bartlett FS 2nd, Frankel WN, van den Pol AN, Bloom FE, Gautvik KM, Sutcliffe JG. 1998. The hypocretins: hypothalamus-specific peptides with neuroexcitatory activity. Proc Natl Acad Sci U S A 95:322–327.
De Parada MP, Parada MA, Rada P, Hernandez L, Hoebel BG. 2000. Dopamine-acetylcholine interaction in the rat lateral hypothalamus in the control of locomotion. Pharmacol Biochem Behav 66:227–234.
de Vries GJ, Buijs RM, Swaab DF. 1981. Ontogeny of the vasopressinergic neurons of the suprachiasmatic nucleus and their extrahypothalamic projections in the rat brain—presence of a sex difference in the lateral septum. Brain Res 218:67–78.
Dean P, Mitchell IJ, Redgrave P. 1988. Responses resembling defensive behaviour produced by microinjection of glutamate into superior colliculus of rats. Neuroscience 24:501–510.
Dean P, Redgrave P, Westby GW. 1989. Event or emergency? Two response systems in the mammalian superior colliculus. Trends Neurosci 12:137–147.
Del-Fava F, Hasue RH, Ferreira JG, Shammah-Lagnado SJ. 2007. Efferent connections of the rostral linear nucleus of the ventral tegmental area in the rat. Neuroscience 145:1059–1076.
Dielenberg RA, Hunt GE, McGregor IS. 2001b. "When a rat smells a cat": the distribution of Fos immunoreactivity in rat brain following exposure to a predatory odor. Neuroscience 104:1085–1097.
Diorio D, Viau V, Meaney MJ. 1993. The role of the medial prefrontal cortex (cingulate gyrus) in the regulation of hypothalamic-pituitary-adrenal responses to stress. J Neurosci 13:3839–3847.
Drager UC, Hubel DH. 1975. Responses to visual stimulation and relationship between visual, auditory, and somatosensory inputs in mouse superior colliculus. J Neurophysiol 38:690–713.
Drew T, Cabana T, Rossignol S. 1996. Responses of medullary reticulospinal neurones to stimulation of cutaneous limb nerves during locomotion in intact cats. Exp Brain Res 111:153–168.
Ennis M, Xu SJ, Rizvi TA. 1997. Discrete subregions of the rat midbrain periaqueductal gray project to nucleus ambiguus and the periambigual region. Neuroscience 80: 829–845.
Fay RA, Norgren R. 1997. Identification of rat brainstem multisynaptic connections to the oral motor nuclei using pseudorabies virus. III. Lingual muscle motor systems. Brain Res Brain Res Rev 25:291–311.
Feldman S, Conforti N. 1985. Modifications of adrenocortical responses following frontal cortex simulation in rats with hypothalamic deafferentations and medial forebrain bundle lesions. Neuroscience 15:1045–1047.
Felsen G, Mainen ZF. 2008. Neural substrates of sensory-guided locomotor decisions in the rat superior colliculus. Neuron 60:137–148.
Fernandez De Molina A, Hunsperger RW. 1962. Organization of the subcortical system governing defence and flight reactions in the cat. J Physiol 160:200–213.
Fields HL, Clanton CH, Anderson SD. 1977. Somatosensory properties of spinoreticular neurons in the cat. Brain Res 120:49–66.
Franklin KBJ, Paxinos G. 2008. The mouse brain in stereotaxic coordinates. San Diego: Academic Press.
Furigo IC, de Oliveira WF, de Oliveira AR, Comoli E, Baldo MV, Mota-Ortiz SR, Canteras NS. 2010. The role of the superior colliculus in predatory hunting. Neuroscience 165:1–15.
Gabbott PL, Warner TA, Jays PR, Salway P, Busby SJ. 2005. Prefrontal cortex in the rat: projections to subcortical autonomic, motor, and limbic centers. J Comp Neurol 492:145–177.
Gonzalo-Ruiz A, Leichnetz GR, Hardy SG. 1990. Projections of the medial cerebellar nucleus to oculomotor-related midbrain areas in the rat: an anterograde and retrograde HRP study. J Comp Neurol 296:427–436.
Goto M, Canteras NS, Burns G, Swanson LW. 2005. Projections from the subfornical region of the lateral hypothalamic area. J Comp Neurol 493:412–438.
Gross CT, Canteras NS. 2012. The many paths to fear. Nat Rev Neurosci 13:651–658.
Hahn JD, Swanson LW. 2010. Distinct patterns of neuronal inputs and outputs of the juxtaparaventricular and

suprafornical regions of the lateral hypothalamic area in the male rat. Brain Res Rev 64:14–103.
Hahn JD, Swanson LW. 2012. Connections of the lateral hypothalamic area juxtadorsomedial region in the male rat. J Comp Neurol 520:1831–1890.
Hahn JD, Swanson LW. 2015. Connections of the juxtaventromedial region of the lateral hypothalamic area in the male rat. Front Syst Neurosci 9:66.
Hara J, Beuckmann CT, Nambu T, Willie JT, Chemelli RM, Sinton CM, Sugiyama F, Yagami K, Goto K, Yanagisawa M, Sakurai T. 2001. Genetic ablation of orexin neurons in mice results in narcolepsy, hypophagia, and obesity. Neuron 30:345–354.
Hattox AM, Priest CA, Keller A. 2002. Functional circuitry involved in the regulation of whisker movements. J Comp Neurol 442:266–276.
Hermann GE, Holmes GM, Rogers RC, Beattie MS, Bresnahan JC. 2003. Descending spinal projections from the rostral gigantocellular reticular nuclei complex. J Comp Neurol 455:210–221.
Hess WR. 1947. Vegetative Funktionen und Zwischenhirn. Helv Physiol Pharmakol Acta Suppl IV:1–89.
Hess WR. 1957. The functional organization of the diencephalon. New York: Grune & Stratton.
Hess WR, Brügger M. 1943. Das subkortikale Zentrum der affektive Abwehrreaktion. Helv Phyiol Acta, 1:32–52.
Holstege G. 1987. Some anatomical observations on the projections from the hypothalamus to brainstem and spinal cord: an HRP and autoradiographic tracing study in the cat. J Comp Neurol 260:98–126.
Holstege JC, Kuypers HG. 1982. Brain stem projections to spinal motoneuronal cell groups in rat studied by means of electron microscopy autoradiography. Prog Brain Res 57: 177–183.
Hosoya Y, Matsushita M. 1981. Brainstem projections from the lateral hypothalamic area in the rat, as studied with autoradiography. Neurosci Lett 24:111–116.
Hunsperger RW. 1956. Affekreaktionen auf elektrische Reizung im Hirnstamm der Katze. Helv Physiol Acta 14:70–92.
Iigaya K, Horiuchi J, McDowall LM, Dampney RA. 2010. Topographical specificity of regulation of respiratory and renal sympathetic activity by the midbrain dorsolateral periaqueductal gray. Am J Physiol Regul Integr Comp Physiol 299:R853–R861.
Jänig W. 2006. Integrative action of the autonomic nervous system: neurobiology of homeostasis. New York: Cambridge University Press.
Jian BJ, Acernese AW, Lorenzo J, Card JP, Yates BJ. 2005. Afferent pathways to the region of the vestibular nuclei that participates in cardiovascular and respiratory control. Brain Res 1044:241–250.
Johnson PL, Molosh A, Fitz SD, Truitt WA, Shekhar A. 2012. Orexin, stress, and anxiety/panic states. Prog Brain Res 198:133–161.
Jordan D. 1990. Autonomic changes in affective behavior. In: Loewy ADS, editor. Central regulation of autonomic functions. New York: Oxford University Press. p 349–366.
Kabat H, Anson BJ, Magoun HW, Ranson SW. 1935. Stimulation of the hypothalamus with special reference to its effect on gastro-intestinal motility. Am J Physiol 112: 214–226.
Kaestner KH, Lee KH, Schlondorff J, Hiemisch H, Monaghan AP, Schutz G. 1993. Six members of the mouse forkhead gene family are developmentally regulated. Proc Natl Acad Sci U S A 90:7628–7631.
Karplus JP, Kreidl A. 1910. Gehirn und Sympathikus: II. Ein Sympathikus Zentrum im Zwischenhirn. Pflügers Arch Ges Physiol Menschen Tiere 135:401–416.
Kita H, Oomura Y. 1982. An HRP study of the afferent connections to rat lateral hypothalamic region. Brain Res Bull 8:63–71.
Knuepfer MM, Holt IL. 1991. Effects of electrical and chemical stimulation of nucleus raphe magnus on responses to renal nerve stimulation. Brain Res 543:327–334.
Koolhaas JM, Everts H, de Ruiter AJ, de Boer SF, Bohus B. 1998. Coping with stress in rats and mice: differential peptidergic modulation of the amygdala–lateral septum complex. Prog Brain Res 119:437–448.
Korte SM, Jaarsma D, Luiten PG, Bohus B. 1992. Mesencephalic cuneiform nucleus and its ascending and descending projections serve stress-related cardiovascular responses in the rat. J Auton Nerv Syst 41:157–176.
Krout KE, Mettenleiter TC, Loewy AD. 2003. Single CNS neurons link both central motor and cardiosympathetic systems: a double-virus tracing study. Neuroscience 118:853–866.
Kunzle H. 1973. The topographic organization of spinal afferents to the lateral reticular nucleus of the cat. J Comp Neurol 149:103–115.
Kunzle H, Wiesendanger M. 1974. Pyramidal connections to the lateral reticular nucleus in the cat: a degeneration study. Acta Anat 88:104–114.
Larson C. 1991. Activity of PAG neurons during conditioned vocalization in the macaque monkey. In: Depaulis A, Bandler R, editors. The midbrain periaqueductal gray matter. New York: Springer. p 23–40.
Liang H, Duan D, Watson C, Paxinos G. 2013. Projections from the paralemniscal nucleus to the spinal cord in the mouse. Brain Struct Funct 218:1307–1316.
Lin D, Boyle MP, Dollar P, Lee H, Lein ES, Perona P, Anderson DJ. 2011. Functional identification of an aggression locus in the mouse hypothalamus. Nature 470:221–226.
Lin L, Faraco J, Li R, Kadotani H, Rogers W, Lin X, Qiu X, de Jong PJ, Nishino S, Mignot E. 1999. The sleep disorder canine narcolepsy is caused by a mutation in the hypocretin (orexin) receptor 2 gene. Cell 98:365–376.
Lumb BM, Morrison JFB. 1984. Convergence of visceral and somatic information on to identified reticulospinal and raphe-spinal neurons in the rat. J Physiol Lond 357:P33–P33.
Mantyh PW. 1982. Forebrain projections to the periaqueductal gray in the monkey, with observations in the cat and rat. J Comp Neurol 206:146–158.
Mason P. 2005. Ventromedial medulla: pain modulation and beyond. J Comp Neurol 493:2–8.
May PJ. 2006. The mammalian superior colliculus: laminar structure and connections. Prog Brain Res 151:321–378.
McHaffie JG, Kao CQ, Stein BE. 1989. Nociceptive neurons in rat superior colliculus: response properties, topography, and functional implications. J Neurophysiol 62:510–525.
Merker BH. 1980. The sentinel hypothesis: a role for the mammalian superior colliculus. Cambridge, MA: Department of Psychology, Massachusetts Institute of Technology.
Miranda-Paiva CM, Ribeiro-Barbosa ER, Canteras NS, Felicio LF. 2003. A role for the periaqueductal grey in opioidergic inhibition of maternal behaviour. Eur J Neurosci 18: 667–674.
Mizuno N, Mochizuki K, Akimoto C, Matsushima R, Sasaki K. 1973. Projections from the parietal cortex to the brain stem nuclei in the cat, with special reference to the parietal cerebro-cerebellar system. J Comp Neurol 147:511–522.
Morest DK. 1961. Connexions of the dorsal tegmental nucleus in rat and rabbit. J Anat 95:229–246.
Morest DK, Sutin J. 1961. Ascending pathways from an osmotically sensitive region of the medulla oblongata. Exp Neurol 4:413–423.

Morin F, Kennedy DT, Gardner E. 1966. Spinal afferents to the lateral reticular nucleus. I. An histological study. J Comp Neurol 126:511–522.

Morin LP, Blanchard JH. 2005. Descending projections of the hamster intergeniculate leaflet: relationship to the sleep/arousal and visuomotor systems. J Comp Neurol 487:204–216.

Motta SC, Goto M, Gouveia FV, Baldo MV, Canteras NS, Swanson LW. 2009. Dissecting the brain's fear system reveals the hypothalamus is critical for responding in subordinate conspecific intruders. Proc Natl Acad Sci U S A 106:4870–4875.

Nagata T, Suzuki H, Zhang R, Ozaki M, Kawakami Y. 2003. Mechanical stimulation activates small fiber mediated nociceptive responses in the nucleus gigantocellularis. Exp Brain Res 149:505–511.

Nakao H. 1958. Emotional behavior produced by hypothalamic stimulation. Am J Physiol 194:411–418.

Netzer F, Bernard JF, Verberne AJ, Hamon M, Camus F, Benoliel JJ, Sevoz-Couche C. 2011. Brain circuits mediating baroreflex bradycardia inhibition in rats: an anatomical and functional link between the cuneiform nucleus and the periaqueductal grey. J Physiol 589:2079–2091.

Nishino S, Ripley B, Overeem S, Lammers GJ, Mignot E. 2000. Hypocretin (orexin) deficiency in human narcolepsy. Lancet 355:39–40.

Otake K, Nakamura Y. 1998. Single midline thalamic neurons projecting to both the ventral striatum and the prefrontal cortex in the rat. Neuroscience 86:635–649.

Paxinos GCRW, Carrive P, Kirkcaldie MTK, Ashwell KWS. 2009. Chemoarchitectonic atlas of the rat brain. San Diego: Elsevier Academic Press.

Pelosi GG, Tavares RF, Correa FM. 2006. Rostrocaudal somatotopy in the neural connections between the lateral hypothalamus and the dorsal periaqueductal gray of the rat brain. Cell Mol Neurobiol 26:635–643.

Peterson BW, Franck JI, Daunton NG. 1976. Changes in responses of medial pontomedullary reticular neurons during repetitive cutaneous, vestibular, cortical, and tectal stimulation. J Neurophysiol 39:564–581.

Peyron C, Tighe DK, van den Pol AN, de Lecea L, Heller HC, Sutcliffe JG, Kilduff TS. 1998. Neurons containing hypocretin (orexin) project to multiple neuronal systems. J Neurosci 18:9996–10015.

Qu D, Ludwig DS, Gammeltoft S, Piper M, Pelleymounter MA, Cullen MJ, Mathes WF, Przypek R, Kanarek R, Maratos-Flier E. 1996. A role for melanin-concentrating hormone in the central regulation of feeding behaviour. Nature 380:243–247.

Radyushkin K, Anokhin K, Meyer BI, Jiang Q, Alvarez-Bolado G, Gruss P. 2005. Genetic ablation of the mammillary bodies in the Foxb1 mutant mouse leads to selective deficit of spatial working memory. Eur J Neurosci 21: 219–229.

Ranson SW, Magoun HW. 1933. Respiratory and pupillary reactions induced by electrical stimulation of the hypothalamus. Arch Neurol Psychiatry 29:1179–1194.

Redgrave P, Dean P, Mitchell IJ, Odekunle A, Clark A. 1988. The projection from superior colliculus to cuneiform area in the rat. I. Anatomical studies. Exp Brain Res 72:611–625.

Rhoades RW, Mooney RD, Rohrer WH, Nikoletseas MM, Fish SE. 1989. Organization of the projection from the superficial to the deep layers of the hamster's superior colliculus as demonstrated by the anterograde transport of *Phaseolus vulgaris* leucoagglutinin. J Comp Neurol 283:54–70.

Rieck RW, Huerta MF, Harting JK, Weber JT. 1986. Hypothalamic and ventral thalamic projections to the superior colliculus in the cat. J Comp Neurol 243:249–265.

Robinson FR, Phillips JO, Fuchs AF. 1994. Coordination of gaze shifts in primates: brainstem inputs to neck and extraocular motoneuron pools. J Comp Neurol 346:43–62.

Roeling TA, Veening JG, Peters JP, Vermelis ME, Nieuwenhuys R. 1993. Efferent connections of the hypothalamic "grooming area" in the rat. Neuroscience 56:199–225.

Roeling TA, Veening JG, Kruk MR, Peters JP, Vermelis ME, Nieuwenhuys R. 1994a. Efferent connections of the hypothalamic "aggression area" in the rat. Neuroscience 59:1001–1024.

Roeling TAP, Veening JG, Kruk MR, Peters JPW, Vermelis MEJ, Nieuwenhuys R. 1994b. Efferent connections of the hypothalamic aggression area in the rat. Neuroscience 59:1001–1024.

Sakurai T, Amemiya A, Ishii M, Matsuzaki I, Chemelli RM, Tanaka H, Williams SC, Richardson JA, Kozlowski GP, Wilson S, Arch JR, Buckingham RE, Haynes AC, Carr SA, Annan RS, McNulty DE, Liu WS, Terrett JA, Elshourbagy NA, Bergsma DJ, Yanagisawa M. 1998a. Orexins and orexin receptors: a family of hypothalamic neuropeptides and G protein-coupled receptors that regulate feeding behavior. Cell 92:573–585.

Sakurai T, Amemiya A, Ishii M, Matsuzaki I, Chemelli RM, Tanaka H, Williams SC, Richarson JA, Kozlowski GP, Wilson S, Arch JR, Buckingham RE, Haynes AC, Carr SA, Annan RS, McNulty DE, Liu WS, Terrett JA, Elshourbagy NA, Bergsma DJ, Yanagisawa M. 1998b. Orexins and orexin receptors: a family of hypothalamic neuropeptides and G protein-coupled receptors that regulate feeding behavior. Cell 92:1 page following 696.

Saper CB. 2004. Hypothalamus. In: Paxinos G, Mai JK, editors. The human nervous system. San Diego: Elsevier Academic Press. p 514–550.

Saper CB, Swanson LW, Cowan WM. 1979. An autoradiographic study of the efferent connections of the lateral hypothalamic area in the rat. J Comp Neurol 183:689–706.

Schulz B, Lambertz M, Schulz G, Langhorst P. 1983. Reticular formation of the lower brainstem. A common system for cardiorespiratory and somatomotor functions: discharge patterns of neighboring neurons influenced by somatosensory afferents. J Auton Nerv Syst 9:433–449.

Schwaller B, Dick J, Dhoot G, Carroll S, Vrbova G, Nicotera P, Pette D, Wyss A, Bluethmann H, Hunziker W, Celio MR. 1999. Prolonged contraction–relaxation cycle of fast-twitch muscles in parvalbumin knockout mice. Am J Physiol 276:C395–C403.

Skofitsch G, Jacobowitz DM, Zamir N. 1985. Immunohistochemical localization of a melanin concentrating hormone-like peptide in the rat brain. Brain Res Bull 15: 635–649.

Slomianka L, West MJ. 2005. Estimators of the precision of stereological estimates: an example based on the CA1 pyramidal cell layer of rats. Neuroscience 136:757–767.

Spencer SE, Sawyer WB, Loewy AD. 1989. Cardiovascular effects produced by L-glutamate stimulation of the lateral hypothalamic area. Am J Physiol 257:H540–H552.

Stein BE, Stanford TR, Rowland BA. 2009. The neural basis of multisensory integration in the midbrain: its organization and maturation. Hear Res 258:4–15.

Steriade M, Sakai K, Jouvet M. 1984. Bulbo-thalamic neurons related to thalamocortical activation processes during paradoxical sleep. Exp Brain Res 54:463–475.

Su HS, Bentivoglio M. 1990. Thalamic midline cell populations projecting to the nucleus accumbens, amygdala, and hippocampus in the rat. J Comp Neurol 297:582–593.

Sukikara M, Mota-Ortiz S, Baldo M, Felicio L, Canteras N. 2006. A role for the periaqueductal gray in switching adaptive behavioral responses. J Neurosci 26:2583–2589.

Sutcliffe JG, de Lecea L. 2000. The hypocretins: excitatory neuromodulatory peptides for multiple homeostatic systems, including sleep and feeding. J Neurosci Res 62: 161–168.

Tang PC, Gernandt BE. 1969. Autonomic responses to vestibular stimulation. Exp Neurol 24:558–578.

Thies R. 1985. Activation of lumbar spinoreticular neurons by stimulation of muscle, cutaneous and sympathetic afferents. Brain Res 333:151–155.

Van Bockstaele EJ, Aston-Jones G. 1992. Distinct populations of neurons in the ventromedial periaqueductal gray project to the rostral ventral medulla and abducens nucleus. Brain Res 576:59–67.

Van Bockstaele EJ, Pieribone VA, Aston-Jones G. 1989. Diverse afferents converge on the nucleus paragigantocellularis in the rat ventrolateral medulla: retrograde and anterograde tracing studies. J Comp Neurol 290:561–584.

Van Bockstaele EJ, Aston-Jones G, Pieribone VA, Ennis M, Shipley MT. 1991. Subregions of the periaqueductal gray topographically innervate the rostral ventral medulla in the rat. J Comp Neurol 309:305–327.

Van der Werf YD, Witter MP, Groenewegen HJ. 2002. The intralaminar and midline nuclei of the thalamus. Anatomical and functional evidence for participation in processes of arousal and awareness. Brain Res Brain Res Rev 39:107–140.

Van Eden CG, Buijs RM. 2000. Functional neuroanatomy of the prefrontal cortex: autonomic interactions. Prog Brain Res 126:49–62.

VanderHorst VG, Ulfhake B. 2006. The organization of the brainstem and spinal cord of the mouse: relationships between monoaminergic, cholinergic, and spinal projection systems. J Chem Neuroanat 31:2–36.

Veenema AH, Neumann ID. 2008. Central vasopressin and oxytocin release: regulation of complex social behaviours. Prog Brain Res 170:261–276.

Veening JG, Te Lie S, Posthuma P, Geeraedts LM, Nieuwenhuys R. 1987. A topographical analysis of the origin of some efferent projections from the lateral hypothalamic area in the rat. Neuroscience 22:537–551.

Villalobos J, Ferssiwi A. 1987a. The differential ascending projections from the anterior, central and posterior regions of the lateral hypothalamic area: an autoradiographic study. Neurosci Lett 81:89–94.

Villalobos J, Ferssiwi A. 1987b. The differential descending projections from the anterior, central and posterior regions of the lateral hypothalamic area: an autoradiographic study. Neurosci Lett 81:95–99.

Walker SC, Winn P. 2007. An assessment of the contributions of the pedunculopontine tegmental and cuneiform nuclei to anxiety and neophobia. Neuroscience 150:273–290.

Wasman M, Flynn JP. 1962. Directed attack elicited from hypothalamus. Arch Neurol 6:220–227.

West MJ, Slomianka L, Gundersen HJ. 1991. Unbiased stereological estimation of the total number of neurons in thesubdivisions of the rat hippocampus using the optical fractionator. Anat Rec 231:482–497.

Wiberg M. 1992. Reciprocal connections between the periaqueductal gray matter and other somatosensory regions of the cat midbrain: a possible mechanism of pain inhibition. Upsala J Med Sci 97:37–47.

Wolf A, Ryu S. 2013. Specification of posterior hypothalamic neurons requires coordinated activities of Fezf2, Otp, Sim1a and Foxb1.2. Development 140:1762–1773.

Wolf G, Sutin J. 1966. Fiber degeneration after lateral hypothalamic lesions in the rat. J Comp Neurol 127:137–156.

Yates BJ, Stocker SD. 1998. Integration of somatic and visceral inputs by the brainstem: functional considerations. Exp Brain Res 119:269–275.

Zhao T, Zhou X, Szabo N, Leitges M, Alvarez-Bolado G. 2007. Foxb1-driven Cre expression in somites and the neuroepithelium of diencephalon, brainstem, and spinal cord. Genesis 45:781–787.

Zhao T, Szabo N, Ma J, Luo L, Zhou X, Alvarez-Bolado G. 2008. Genetic mapping of Foxb1-cell lineage shows migration from caudal diencephalon to telencephalon and lateral hypothalamus. Eur J Neurosci 28:1941–1955.

Zhou J, Nannapaneni N, Shore S. 2007. Vessicular glutamate transporters 1 and 2 are differentially associated with auditory nerve and spinal trigeminal inputs to the cochlear nucleus. J Comp Neurol 500:777–787.